AMEGHINIANA
A GONDWANAN PALEONTOLOGICAL JOURNAL

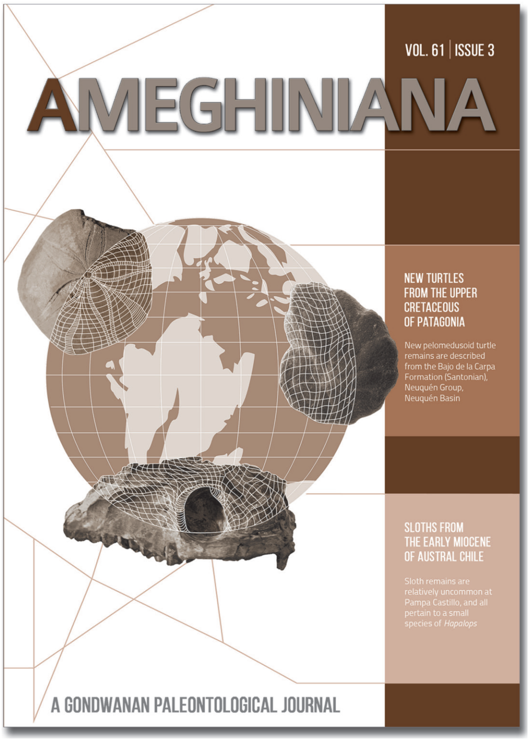

EARLY MIOCENE SLOTH (FOLIVORA) REMAINS FROM PAMPA CASTILLO, SOUTHERN CHILE, INCLUDING A NATURAL CRANIAL ENDOCAST

NATHANAEL J. LEE[1]
JOHN J. FLYNN[2]
ANDRÉ R WYSS[3]
DARIN A. CROFT[4]

[1]Department of Biology, Case Western Reserve University, 10900 Euclid Ave., Cleveland, Ohio, 44106, USA.
[2]Division of Paleontology, American Museum of Natural History, Central Park West at 79th St., New York, NY 10024-5192, USA.
[3]Department of Earth Science, University of California - Santa Barbara, Santa Barbara, CA 93106, USA.
[4]Department of Anatomy, Case Western Reserve University, 10900 Euclid Ave., Cleveland, Ohio, 44106-4930, USA.

Submitted: 28 March 2024 - **Accepted:** 26 June 2024 - **Published:** 08 August 2024

To cite this article: Nathanael J. Lee, John J. Flynn, André R Wyss, & Darin A. Croft (2024). Early Miocene sloth (Folivora) remains from Pampa Castillo, Southern Chile, including a natural cranial endocast. *Ameghiniana*, *61*(3), 148–169.

To link to this article: http://dx.doi.org/10.5710/AMGH.26.06.2024.3603

NEW TURTLES FROM THE UPPER CRETACEOUS OF PATAGONIA

New pelomedusoid turtle remains are described from the Bajo de la Carpa Formation (Santonian), Neuquén Group, Neuquén Basin

SLOTHS FROM THE EARLY MIOCENE OF AUSTRAL CHILE

Sloth remains are relatively uncommon at Pampa Castillo, and all pertain to a small species of *Hapalops*

ARTICLES

AMEGHINIANA - 2024 - Volume 61(3): 148–169

ISSN 0002-7014

EARLY MIOCENE SLOTH (FOLIVORA) REMAINS FROM PAMPA CASTILLO, SOUTHERN CHILE, INCLUDING A NATURAL CRANIAL ENDOCAST

NATHANAEL J. LEE[1], JOHN J. FLYNN[2], ANDRÉ R. WYSS[3], and DARIN A. CROFT[4]

[1] Department of Biology, Case Western Reserve University, 10900 Euclid Ave., Cleveland, Ohio, 44106, USA. *nathanaelee14@gmail.com*

[2] Division of Paleontology, American Museum of Natural History, Central Park West at 79th St., New York, NY 10024-5192, USA. *jflynn@amnh.org*

[3] Department of Earth Science, University of California - Santa Barbara, Santa Barbara, CA 93106, USA. *wyss@geol.ucsb.edu*

[4] Department of Anatomy, Case Western Reserve University, 10900 Euclid Ave., Cleveland, Ohio, 44106-4930, USA. *dcroft@case.edu*

Abstract. The Pampa Castillo site in southern Chile has yielded a wide variety of Early Miocene (Burdigalian; Santacrucian SALMA; ~18-million-year-old) mammal remains including metatherians, rodents, xenarthrans, and South American native ungulates. Here, we document the folivoran (sloth) remains from the Pampa Castillo Fauna: a slightly distorted natural cranial endocast lacking the olfactory bulbs and four other specimens that together include a partial molariform tooth, a nearly complete astragalus, and various partial postcranial bones. All Pampa Castillo sloth specimens are similar in size and morphology, and we refer them to a single species of the megatherioid genus *Hapalops* primarily based on the astragalus and cranial endocast. The Pampa Castillo *Hapalops* species was relatively small, comparable to Santa Cruz Formation species such as *H. angustipalatus, H. elongatus*, and *H. ruetimeyeri*. We estimate its encephalization quotient at 0.40, close to values for *H. indifferens* and *Eucholoeops ingens* (0.48–0.58), smaller than values for extant sloths (0.68–0.90), and larger than values for Pleistocene sloths (0.16–0.31). The scarcity of sloth specimens at Pampa Castillo (< 1% of identified specimens) characterizes several other contemporaneous sites in southern South America (*e.g.*, the Pinturas Formation and Upper Faunal Zone of Gran Barranca in Argentina and Sierra Baguales in Chile) and contrasts sharply with their abundance in the Santa Cruz Formation, likely reflecting some combination of climatic and/or vegetational differences, perhaps related to temporal and/or biogeographic variation. To our knowledge, the specimen from Pampa Castillo is the first described natural endocast from an extinct mammal from Chile.

Key words. Astragalus. Encephalization Quotient (EQ). *Hapalops*. Neogene. Pilosa. Phyllophaga. Santacrucian. Xenarthra.

Resumen. RESTOS DE PEREZOSOS (FOLIVORA) DEL MIOCENO TEMPRANO DE PAMPA CASTILLO, CHILE AUSTRAL, INCLUYENDO UN MOLDE ENCOCRANEANO NATURAL. El sitio de Pampa Castillo en el sur de Chile ha producido una amplia variedad de restos de mamíferos del Mioceno Temprano (Burdigaliano; Edad-mamífero Santacrucense; ~18 millones de años), incluyendo metaterios, roedores, xenartros y ungulados nativos sudamericanos. Aquí, documentamos los restos de los Folivora (perezosos) de la fauna de Pampa Castillo: un molde endocraneano natural que carece de los bulbos olfatorios y está ligeramente distorsionado y otros cuatro especímenes que en conjunto incluyen un diente molariforme parcial, un astrágalo casi completo, y varios huesos postcraneales parciales. Todos los especímenes de perezosos de Pampa Castillo son similares en tamaño y morfología, y los referimos a una sola especie del género megaterioideo *Hapalops*, basado principalmente en el astrágalo y el molde endocraneano. La especie de *Hapalops* de Pampa Castillo era relativamente pequeña, comparable a especies de la Formación Santa Cruz como *H. angustipalatus*, *H. elongatus* y *H. ruetimeyeri*. Estimamos su cociente de encefalización en 0,40, cercano a los valores de *H. indifferens* y *Eucholoeops ingens* (0,48–0,58), menor que los valores de los perezosos actuales (0,68–0,90) y mayor que los valores de perezosos pleistocénicos (0,16–0,31). La escasez de especímenes de perezosos en Pampa Castillo (<1% de los especímenes identificados) caracteriza a varios otros sitios contemporáneos del sur de Sudamérica (por ejemplo, la Formación Pinturas y la Upper Fossil Zone de Gran Barranca en Argentina y Sierra Baguales en Chile) y contrasta marcadamente con su abundancia en la Formación Santa Cruz, probablemente reflejando alguna combinación de diferencias climáticas y/o florísticas, tal vez relacionadas con variaciones temporales y/o biogeográficas. Hasta donde sabemos, el ejemplar de Pampa Castillo es el primer molde endocraneano natural descripto de un mamífero extinto de Chile.

Palabras clave. Astrágalo. Cociente de Encefalización (EQ). *Hapalops*. Neógeno. Phyllophaga. Pilosa. Santacrucense. Xenarthra.

The pre-Pleistocene fossil record of sloths (folivorans/phyllophagans) in Chile is long but relatively sparse. The geologically oldest record is *Pseudoglyptodon chilensis* from the early Oligocene (Rupelian; Tinguiririan South American Land Mammal 'Age' or **SALMA**; ~32 Ma) Tinguiririca Fauna in the Abanico Formation at Termas del Flaco (McKenna *et al.*, 2006), located in central Chile ~175 km southeast of Santiago (~35° S; see Wyss *et al.*, 1993, 1994, 2018; Flynn *et al.*, 2003, 2012; Croft *et al.*, 2008). This is among the earliest records of sloths in South America, exceeded only by slightly older (Priabonian; Mustersan SALMA; ~37 Ma) remains of an unidentified species of *Pseudoglyptodon* from

Chubut, Argentina (McKenna *et al.*, 2006; Gaudin & Croft, 2015). Other possible Paleogene sloth remains from Chile consist of undescribed Abanico Formation specimens from several sites in valleys south of the Río Tinguiririca that are either late Oligocene or Early Miocene in age (Flynn *et al.*, 2012).

Most folivoran remains from Chile are late Early Miocene in age (*i.e.*, Burdigalian; Santacrucian or Friasian/Colloncuran SALMA) and come from the southernmost portion of the country (Aysén and Magallanes regions, south of ~44° S). Simpson (1941) described a partial mylodontid cranium from the Palomares Formation (Magallanes Region) and designated it as the holotype of a new species, *Nematherium birdi*. The Palomares Formation may correspond to the well-known Santa Cruz Formation of southern Argentina, which is predominantly late Early Miocene in age, at least near the Atlantic Coast (Fleagle *et al.*, 2012; Perkins *et al.*, 2012). The Santa Cruz Formation is exposed at other sites in southern Chile such as Sierra Baguales (Bostelmann *et al.*, 2013), where remains have been preliminarily identified as corresponding to two species, one similar to *Eucholoeops* Ameghino, 1887 and *Pseudortotherium* and another similar to *Pelecyodon* Ameghino, 1891c and *Hapalops* Ameghino, 1887 (Bostelmann & Oyarzún, 2013).

Kraglievich (1930) identified a partial edentulous sloth cranium from the Río Frías Formation at Alto Río Cisnes (Aysén Region; Marshall & Salinas, 1990) as a new species of megatheriid, *Megathericulus friasensis*. Later, Bondesio *et al.* (1980) added the mylodontid *Neonematherium* to the list of Río Frías Formation mammals. However, those authors did not provide a rationale for their identification and, to our knowledge, it has been neither substantiated nor refuted by subsequent workers. The age of *M. friasensis* and other 'Friasian' *sensu stricto* mammals is not well constrained, though a single age of "about 16.5 Ma" comes from the lower levels of the formation (Flynn & Swisher, 1995: p. 325). This suggests that Río Frías fossils (Friasian SALMA *sensu stritco*) are slightly younger than most Santa Cruz Formation fossils: latest Early Miocene (Burdigalian) or perhaps early Middle Miocene (Langhian).

Flynn *et al.* (2008) reported a mandible of *Nematherium* from the Cura Mallín Formation at Laguna del Laja (Biobío Region), a site *ca.* 800 km north of Río Cisnes. The specimen was recovered from outcrops at Estero Correntoso that correlate with a ^{40}Ar/^{39}Ar date of 19.80±0.40 Ma (Flynn *et al.*, 2008), indicating a late Early Miocene age that is slightly older than or contemporaneous with most Santa Cruz Formation fossils (Fleagle *et al.*, 2012; Perkins *et al.*, 2012). Solórzano *et al.* (2021) referred a partial dentary with several tooth fragments from Laguna del Laja to *Hapalops* sp. The specimen was collected from Cerro Campamento, a locality of similar age to Estero Correntoso (Flynn *et al.*, 2008).

The Middle Miocene record of sloths in Chile is unknown due to a gap in the fossil record between late Early Miocene sites in the south and Late Miocene ones in the north. The early Late Miocene (Tortonian) record is sparse, consisting only of undescribed remains of an indeterminate sloth from Caragua, northernmost Chile (~18.5° S; Arica and Parinacota regions; Bostelmann *et al.*, 2018; see also Flynn *et al.*, 2005; Montoya-Sanhueza *et al.*, 2017; Campos-Medina *et al.*, 2023).

All securely identified late Late Miocene (Messinian) and Pliocene sloth remains from Chile pertain to the semiaquatic sloth *Thalassocnus*, which was first described from the Pisco Formation of southern Peru (Muizon & McDonald, 1995). Chilean *Thalassocnus* remains were first reported by Canto *et al.* (2008) from Late Miocene (Messinian) or possibly Pliocene levels of the Bahía Inglesa Formation of the Atacama Region (~27° S). Additional remains of *Thalassocnus* from this formation have been reported by others (Pyenson *et al.*, 2014; Peralta-Prato & Solórzano, 2019). More southerly remains of *Thalassocnus* were described by De Los Arcos *et al.* (2017) from the Coquimbo Formation (~30° S; Coquimbo Region) and Horcón Formation (~33° S; Valparaíso Region) and are likely similar in age to remains from the Bahía Inglesa Formation. The specimens from Chile represented the only occurrences of *Thalassocnus* outside of Peru prior to the recent report of Quiñones *et al.* (2022), who identified a specimen from the Late Miocene or Pliocene Tafna Formation of northern Argentina (Jujuy Province)

In this contribution, we add to the Chilean folivoran record by describing sloth remains from the late Early Miocene (Burdigalian; Santacrucian SALMA) of Pampa Castillo in southern Chile, a site with a diverse record of terrestrial fossil mammals that includes metatherians, cingulates, rodents, and South American native ungulates

(“SANUs”) in addition to folivorans (Flynn *et al.*, 2002b; McGrath *et al.*, 2020, 2022, 2023). This study began as the undergraduate Capstone project of the first author (NJL), which focused on describing and identifying SGOPV 2388, a natural endocast from the site that was discovered without any associated osteological or dental remains. Once the specimen was identified as pertaining to a sloth, the study’s scope was expanded to include other undescribed folivoran specimens from Pampa Castillo. To our knowledge, this is the first natural endocast of an extinct mammal to be described from Chile.

Endocasts are indispensable evidence for documenting brain evolution and have been described and analyzed in a wide variety of extinct amniotes (see Dozo *et al.*, 2023 for a recent authoritative review). The earliest paleoneurological studies were based on natural endocasts or artificial ones (plaster casts or latex peels of endocranial cavities), but during the past two decades, such studies have mainly relied on ‘virtual’ endocasts: three-dimensional models of the cranial cavity reconstructed from computed tomographic (CT) scans. Studies of endocasts of extinct sloths span more than 150 years, with the vast majority focusing on Pleistocene taxa, including the megatheriid *Megatherium americanum*, the nothrotheriid *Nothrotherium shastense*, and the mylodontids *Glossotherium robustum* Owen, 1842, *Glossotherium wegneri*, *Scelidotherium leptocephalum*, *Lestodon armatus, Paramylodon harlani, Mylodon darwinii*, and *Catonyx tarijensis* (*e.g.*, Pouchet, 1868-1869; Gervais, 1869; Woodward, 1900; Jakob & Onelli, 1913; Stock, 1925; see also Boscaini *et al.*, 2023). However, endocasts of two late Early Miocene genera also have been described: *Hapalops* (Dechaseaux, 1958, 1971; Dozo, 1987) and *Eucholoeops* (Dozo, 1994). Our report adds to the scant pre–Pleistocene paleoneurological record of sloths, and although the specimen pertains to a previously studied genus, it appears to represent a species of *Hapalops* distinct from those the studied by Dechaseaux (1971) and Dozo (1987).

The initial report on the Pampa Castillo Fauna by Flynn *et al.* (2002b) listed 25 genera and 37 species of mammals at the site, nearly half of them rodents. Most taxa and specimens were reported in only general terms, but the palaeothentid metatherians were described in detail, including a new species of *Palaeothentes* (*Palaeothentes smeti*). Several recent papers have updated taxonomic identifications and provided detailed descriptions of the site’s litopterns, which include at least two proterotheriids and a macraucheniid (McGrath *et al.*, 2020), and rodents, which include 18 species from all four major caviomorph clades (McGrath *et al.*, 2022, 2023). Most of the principal taxonomic groups represented in the renowned Santa Cruz Formation of southern Argentina are also present at Pampa Castillo; absences noted by Flynn *et al.* (2002b) include Necrolestidae (*i.e.*, the meridiolestidan *Necrolestes patagonicus*; see Rougier *et al.*, 2012; Wible & Rougier, 2017), Microbiotheriidae (Metatheria: Microbiotheria; see Marshall, 1982; Abello *et al.*, 2012), primates (the platyrrhine *Homunculus patagonicus*; see Kay *et al.*, 2012), Adianthidae (pygmy litopterns; see Cifelli & Soria, 1983), *Notohippus toxodontoides* (a notoungulate closely related to toxodontids; see Hernández Del Pino *et al.*, 2019), and anteaters (*Protamandua*; see Bargo *et al.*, 2012). Flynn *et al.* (2002b) noted the presence of only a single sloth genus at Pampa Castillo, *Hapalops*, in stark contrast to the large diversity of folivorans known from the Santa Cruz Formation in Argentina (roughly a dozen genera representing several families; Bargo *et al.*, 2012, 2019). Our study supports the initial observations of Flynn *et al.* (2002b) by referring all five Pampa Castillo specimens described herein to a single species of *Hapalops*. However, we refine this identification by documenting that the Pampa Castillo *Hapalops* species was relatively small-bodied, precluding its referral to a larger species such as *Hapalops longiceps* Scott, 1903, *Hapalops indifferens* Ameghino, 1887, or *Hapalops platycephalus* Scott, 1903.

Institutional abbreviations. FMNH PM, Fossil Mammal Collection, The Field Museum of Natural History, Chicago, Illinois, USA; **MLP,** Museo de La Plata, Argentina; **MNHN,** Muséum national d’Histoire naturelle, Paris, France; **MPM-PV,** Museo Regional Provincial Padre M.J. Molina, Río Gallegos, Argentina; **SGOPV,** Vertebrate Paleontology Collections, Museo Nacional de Historia Natural, Santiago, Chile; **YPM-VPPU,** Princeton University Vertebrate Paleontology Collection, Yale Peabody Museum, New Haven, Connecticut, USA.

Anatomical abbreviations. arf, anterior rhinal fissure; **eg,** ectosylvian gyrus; **es,** entolateral sulcus; **h,** hypophysis; **lch,** left cerebellar hemisphere; **lg,** lateral gyrus; **ls,** lateral sulcus; **og,** occipital gyrus; **pl,** pyriform lobe; **prf,** posterior rhinal fissure; **ps,** presylvian sulcus; **pss,** pseudosylvian sulcus; **rch,** right cerebellar hemisphere; **sg,** suprasylvian gyrus; **ss,** suprasylvian sulcus; **sss,** superior sagittal sinus; **tf,** transverse fissure; **tl,** temporal lobe; **ve,** vermis.

MATERIAL AND METHODS

Geographic and stratigraphic contexts

The fossil site of Pampa Castillo is located at *ca.* 47° S and 72.4° W, in the southern Chilean province of Aysén, between Lago General Carrera/Buenos Aires (to the north) and Lago Cochrane/Pueyrredón (to the south) (Fig. 1; see Flynn *et al.*, 2002b for details). Pampa Castillo fossils derive from a *ca.* 300 m-thick sequence of Early Miocene fluvial strata located at and above 1,350 m above sea level. These fossiliferous outcrops are on the flanks of a butte located east of a summer grazing pasture known as "Pampa Castillo", after which the site was named (Flynn *et al.*, 2002b). The fossil specimens described herein were collected in 1987, during one of three field seasons at Pampa Castillo that spanned 1986-88 (Flynn *et al.*, 2002b).

The Early Miocene terrestrial deposits at Pampa Castillo are part of a larger sequence of Cenozoic sedimentary and volcanic deposits that are exposed in the area around Meseta Guadal (Encinas *et al.*, 2019), which is located southwest of Pampa Castillo (Flynn *et al.*, 2002b). The most

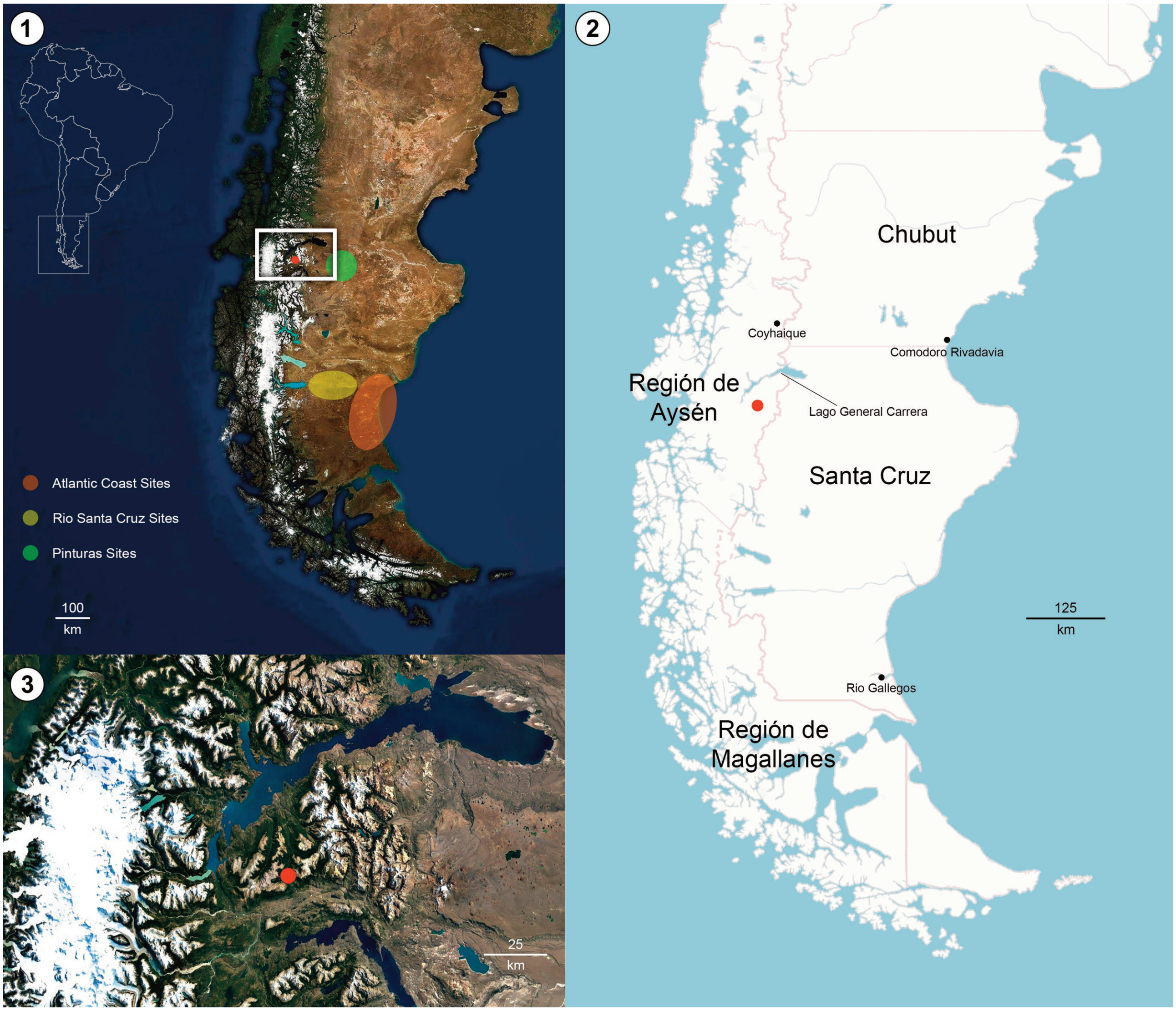

Figure 1. 1–3, Maps of southern South America (satellite, upper left; political map, right) and inset map (lower left) showing the location of Pampa Castillo (red dot) and selected other regions mentioned in the text from which many late Early Miocene (Burdigalian) mammal fossils have been collected (colored ellipses). Images from OpenStreetMap; CalTopo, accessed July 2023.

appropriate geological designation for the fossil-producing strata has been a topic of considerable discussion, but the Pampa Castillo Fauna clearly is late Early Miocene in age (Santacrucian SALMA; summarized in McGrath *et al.*, 2022, 2023). Given the paleontological focus of this contribution, we follow McGrath *et al.* (2023) in referring these strata to an unnamed formation.

The late Early Miocene Santacrucian SALMA age of Pampa Castillo inferred based on its mammals is supported by radioisotopic dates from the area. Encinas *et al.* (2019) inferred a maximum depositional age of *ca.* 19.8±0.4 Ma for the Pampa Castillo sequence based on detrital zircons from a sandstone within the conformably underlying marine Guadal Formation. This is compatible with a U/Pb date of 18.7±0.3 Ma reported earlier by Folguera *et al.* (2018) from a reworked tuff about 10 m above the base of the fossil-producing formation at Meseta Guadal, well below the lowest fossil mammals recovered in the Pampa Castillo stratigraphic sequence. This latter date indicates that the Santacrucian mammals of the Pampa Castillo Fauna are clearly <19 Ma and likely <18.4 Ma (the beginning of the Burdigalian age).

The biochronological and biogeographic implications of Pampa Castillo's abundant and diverse rodents were discussed by McGrath *et al.* (2023). The site is geographically closer to Early Miocene fossil sites in the upper Río Pinturas valley (~130 km; Fig. 1) than to those along the coast and the Río Santa Cruz (> 350 km; Fig. 1). Similarly, Pampa Castillo appears to be closer in age to such 'Pinturan' faunas than 'core Santacrucian' faunas (*sensu* McGrath *et al.*, 2023), including those along the coast of Santa Cruz Province in Argentina. Nevertheless, Pampa Castillo shares more rodent species with younger and more distant Santa Cruz Formation sites than with those that are closer in proximity and age (McGrath *et al.*, 2023). This illustrates that similarities and differences among late Early Miocene faunas of Patagonia are due to a combination of temporal, geographic, and paleoenvironmental factors that have yet to be fully resolved (McGrath *et al.*, 2022, 2023).

Comparative and analytical methods

As a first step toward the taxonomic identification of SGOPV 2388 (the natural endocast), overall size was used to identify candidate clades (generally families) from among those recorded at Early Miocene sites of southern Argentina, including the Santa Cruz Formation. Clades in which all taxa have an estimated body mass < ~1 kg (*e.g.*, Octodontoidea) or > ~100 kg (*e.g.*, Astrapotheria) were discarded as being too small or too large, respectively, to have an endocranial cavity measuring *ca.* 6 cm in length (the estimated size of SGOPV 2388 with olfactory bulbs preserved). Among the remaining clades, endocranial volumes (**EVs**) and endocast characteristics were collected to permit more precise (*i.e.*, genus- and species-level) comparisons.

Endocast volumes for extinct taxa (Table 1) were estimated in one of three ways. In some cases (*e.g.*, most notoungulates), published values were used. In other cases, EV was approximated or bracketed using body mass (**BM**) and data from close relatives. For example, since the estimated BM of the fossil erethizontid rodent *Steiromys duplicatus* (5–10 kg; Candela *et al.*, 2012) is less than that of extant *Erethizon dorsatum* (10–12 kg; Roberts *et al.*, 1985), its EV was assumed to be less than that of *E. dorsatum* (*i.e.*, < 25 cc; Boddy *et al.*, 2012: tab. S1). For remaining taxa, EV was estimated using regressions of EV (for extinct species) and/or brain volume (for extant species) on BM for other members of the same and/or an analogous clade as follows:

The sparassodont metatherian regression equation (**Eq. 1**) was based on EVs from two sparassodonts (*Borhyaena tuberata* and *Sipalocyon gracilis*), supplemented with EVs from seven medium to large (<3 kg) extant dasyurids and the recently extinct thylacine, *Thylacinus cynocephalus* (Supplementary Data S1). We did not include the EVs for the sparassodont *Thylacosmilus atrox* published by Dozo (1994) due to uncertainty about the BM of this species (published estimates range from 48–117 kg; Croft *et al.*, 2018: table S1) and the availability of EVs for two other carnivorous metatherian species of similar size (*Borhyaena tuberata* and *Thylacinus cynocephalus*).

$$\text{Eq. 1: } EV = 0.601(BM) - 1.102$$

The regression equation for Dasypodidae and Peltephilidae **(Eq. 2)** was based on the EVs from eight extant cingulates (Supplementary Data S2).

$$\text{Eq. 2: } EV = 0.635(BM) - 1.146$$

The glyptodont regression equation (**Eq. 3**) was based on published EVs for four glyptodont species (Supplementary Data S3).

TABLE 1. Endocast volumes and body masses of Santacrucian SALMA (late Early Miocene) mammal species (from Croft, 2016, app. 10) between ~1 kg and 100 kg. Endocast volumes in parentheses are estimates based on regression equations; See Materials and Methods for details.

Superfamily or Family	Genus/species	Total Volume (cm^3)	Volume Source	Body Mass (kg)	Body Mass Source
Sparassodonta					
Borhyaenoidea	*Lycopsis torresi*	(30)	Eq. 1	19.4	Ercoli *et al.* (2014)
Borhyaenoidea	*Prothylacynus patagonicus*	(40)	Eq. 1	31.8	Ercoli *et al.* (2014)
Borhyaenidae	*Acrocyon sectorius*	(38)	Eq. 1	28.7	Ercoli *et al.* (2014)
Borhyaenidae	*Arctodictis munizi*	(54)	Eq. 1	51.6	Ercoli *et al.* (2014)
Borhyaenidae	*Borhyaena tuberata*	50	Dozo (1994)	36.4	Ercoli *et al.* (2014)
Hathliacynidae	*Acyon tricuspidatus*	(17)	Eq. 1	8	Ercoli *et al.* (2014)
Hathliacynidae	*Cladosictis patagonica*	(16)	Eq. 1	6.6	Ercoli *et al.* (2014)
Hathliacynidae	*Pseudonotictis pusillus*	(6)	Eq. 1	1.2	Ercoli *et al.* (2014)
Hathliacynidae	*Sipalocyon* spp.	6.82	Gaillard *et al.* (2020)	2.06–2.1	Ercoli *et al.* (2014)
Cingulata					
Dasypodidae	*Paraeutatus distans*	(20–25)[a]	estimate	3.7	González Ruiz (2010)
Dasypodidae	*Proeutatus* spp.	(31)	Eq. 2	7.6–20.6	Vizcaíno *et al.* (2006b)
Dasypodidae	*Prozaedyus* spp.	(7)	Eq. 2	0.8–1.9	Vizcaíno *et al.* (2006b)
Dasypodidae	*Stegotherium tessellatum*	(27)	Eq. 2	11.5	Vizcaíno *et al.* (2006b)
Dasypodidae	*Stenotatus* spp.	(13)	Eq. 2	3.7–3.9	Vizcaíno *et al.* (2006b)
Dasypodidae	*Vetelia puncta*	(50)	Eq. 2	30	Barasoain *et al.* (2021)
Glyptodontidae	*Cochlops* sp.	(68)	Eq. 3	80	Vizcaíno *et al.* (2012)
Glyptodontidae	*Eucinepeltus* sp.	(80)	Eq. 3	115	Vizcaíno *et al.* (2012)
Glyptodontidae	*Propalaehoplophorus* spp.	(66)	Eq. 3	73.4–75.1	Vizcaíno *et al.* (2006a)
Peltephilidae	*Peltephilus* spp.	(24)	Eq. 2	8.3–11.1	Vizcaíno *et al.* (2006b)
Pilosa					
Megatherioidea	*Analcimorphus giganteus*	(96)	Eq. 5	66.9	Toledo *et al.* (2014)
Megatherioidea	*Hapalops elongatus*	(60–78)	Eq. 5	27.7–45	Toledo *et al.* (2014)
Megatherioidea	*Hapalops indifferens*	100	Dozo (1987)	50[b]	
Megatherioidea	*Hapalops longiceps*	(108)	Eq. 5	84	Toledo *et al.* (2014)
Megatherioidea	*Pelecyodon cristatus*	(68)	Eq. 5	(≤ 35)[c]	
Megatherioidea	*Schismotherium fractum*	(77)	Eq. 5	43.7	Toledo *et al.* (2014)
Megatherioidea	*Eucholoeops ingens*	75	Dozo (1994)	44[d]	
Megatheriidae	*Planops martini*	(132)	Eq. 5	(123.2)[e]	
Megatheriidae	*Prepotherium potens*	(132)	Eq. 5	123.2	Toledo *et al.* (2014)
Mylodontidae	*Analcitherium* sp.	(111)	Eq. 5	88.2	Toledo *et al.* (2014)
Mylodontidae	*Nematherium* sp.	(115)	Eq. 5	95	Bargo *et al.* (2012)
Myrmecophagidae	*Protamandua rothi*	(33)	Eq. 4	5.9	Bargo *et al.* (2012)
Primates					
Basal Platyrrhini	*Homunculus patagonicus*	19.5–22.2	Kay *et al.* (2012)	1.5-2.5	Kay *et al.* (2012)
Rodentia					
Cavioidea	*Eocardia fissa*	(18–22)[f]	estimate	2.8	Candela *et al.* (2012)
Cavioidea	*Neoreomys australis*	13.21	Ferreira *et al.* (2020)	5.1	Ferreira *et al.* (2020)
Dinomyidae	*Scleromys* sp.	(14–16)[g]	estimate	1.8	Boivin *et al.* (2021)
Erethizontidae	*Steiromys duplicatus*	(< 25)[h]	estimate	(5–10)	Candela *et al.* (2012)

TABLE 1. Continuation.

Superfamily or Family	Genus/species	Total Volume (cm^3)	Volume Source	Body Mass (kg)	Body Mass Source
Litopterna					
Adianthidae	*Adianthus bucatus*	(23)	Eq. 6	7.4	Croft *et al.* (2020)
Proterotheriidae	*Anisolophus australis*	(56)	Eq. 6	36.6	Cassini *et al.* (2012)
Proterotheriidae	*Diadiaphorus majusculus*	(88)	Eq. 6	82	Croft & Lorente (2021)
Proterotheriidae	*Tetramerorhinus lucarius*	57[i]	Jerison (1973)	37.5	Tejeda-Lara *et al.* (2015)
Proterotheriidae	*Thoatherium minusculum*	42	Radinsky (1981)	21.5	Croft & Lorente (2021)
Notoungulata					
Hegetotheriidae	*Hegetotherium mirabile*	20	Radinsky (1981)	4.5–5.5	Nelson *et al.* (2023)
Hegetotheriidae	*Pachyrukhos* sp.	(< 8)	estimate	1.2–1.6	Nelson *et al.* (2023)
Interatheriidae	*Interatherium extensus*	8[j]	Radinsky (1981)	1.9–2.0	Nelson *et al.* (2023)
Interatheriidae	*Protypotherium australe*	17	Radinsky (1981)	3.5–4.0	Nelson *et al.* (2023)

[a]based on *Cabassous unicinctus* (Boddy *et al.*, 2012: tab. S1); [b]based on cranium length and comparison with *Eucholoeops fronto*; see text for details; [c]equal in size to or smaller than *Hapalops elongatus* based on specimens in Scott (1903); [d]ponderated value for *Eucholoeops* from Toledo *et al.* (2014: tab. 6) adjusted by cranium length; see text for details; [e]comparable to *Prepotherium* based on femora from Hoffstetter (1961); [f]based on *Dasyprocta leporina* (Boddy *et al.*, 2012: tab. S1); [g]based on *Lagidium viscacia* (Boddy *et al.*, 2012: tab. S1); [h]based on *Erethizon dorsatum* (Boddy *et al.*, 2012: tab. S1); [i]listed as *Proterotherium cavum*; [j]listed as *Interatherium robustum*, a junior synonym (Fernández *et al.*, 2023).

Eq. 3: $EV = 0.414(BM) - 0.193$

The Myrmecophagidae regression equation (**Eq. 4**) was based on EVs from two extant species (Supplementary Data S4).

Eq. 4: $EV = 0.760(BM) - 1.343$

The Folivora (sloth) regression equation (**Eq. 5**) was based on EVs from four extant and nine extinct species (Supplementary Data S5). For the two Early Miocene species in our dataset (*Eucholoeops ingens* and *Hapalops indifferens*), we did not use the BM estimates of Toledo *et al.* (2014) because they yield implausible EV/BM relationships for *H. indifferens* and *E. ingens*, with the former having a 33% larger EV (100 cc in *H. indifferens* vs. 75 cc in *E. ingens*; Dozo, 1987, 1994) but 14% smaller BM (56 kg for *H. indifferens* vs. 65 kg for *E. ingens*; Toledo *et al.*, 2014: tabs. 5-6). Instead, we compared the cranial lengths of these two EV specimens (16.3 cm in *H. indifferens*; Dozo, 1987: tab. 2; 15.6 cm in *E. ingens*; Dozo, 1994: tab. 2) and estimated that the individual represented by the *E. ingens* specimen was 14% more massive than the *H. indifferens* individual, assuming geometric similarity (as has been done in other studies of xenarthran paleobiology, *e.g.*, Vizcaíno *et al.*, 2011, 2012). Likewise, the individual represented by the *Eucholoeops* 'cf. *E. fronto*' specimen (MPM-PV 3403, perhaps assignable to *Eucholoeops latifrons*; see De Iuliis *et al.*, 2024) analyzed by Toledo *et al.* (2014) was ~46% more massive than the *E. ingens* specimen studied by Dozo (1994) based on its cranial length of *ca.* 17.7 cm (Bargo *et al.,* 2012: fig. 13.3). Together, these calculations result in a BM estimate of 44 kg for the *E. ingens* specimen and 50 kg for the *H. indifferens* EV specimen.

Eq. 5: $EV = 0.525(BM) - 0.552$

The litoptern equation (**Eq. 6)** was based on EVs from two extinct species (Supplementary Data S6).

Eq. 6: $EV = 0.549(BM) - 0.755$

To calculate the encephalization quotient (**EQ**), we used the following equation from Boddy *et al.* (2012), in which **E** = brain mass (g) and **P** = body mass (g).

$$EQ = E / 0.056 * P^{0.746}$$

The equation is based on data from 930 species of extant mammals, including nine xenarthrans.

For regressions of EV on BM (Eq. 1–6), brain mass in extant species was multiplied by 1.036 (average whole brain specific gravity; Gompertz, 1902) to estimate EV, following other studies (*e.g.,* Kerber & Moraes-Santos, 2021). Similarly, to calculate EQ of extinct species, EV was divided by 1.036 to estimate brain mass.

Nomenclature. Endocast descriptive terminology follows

Boscaini *et al.* (2020a, 2020b, 2023). Osteological terminology follows Gaudin *et al.* (2023). We follow De Iuliis *et al.* (2024) in referring the specimen of *Eucholoeops* studied by Dozo (1994) to *E. ingens*, which they regard as a senior synonym of *E. fronto*.

Measurements. External measurements of Pampa Castillo sloth specimens were made to the nearest 0.05 mm using a Mitutoyo ABSOLUTE digimatic calipers. Photographs were taken using a Pentax K10 digital camera with a Pentax-D FA 50 mm F2.8 macro lens and model AF160FC lens-mounted ring flash. The natural endocast was scanned using a ROMER 7X 3D Scan Arm laser surface scanner, and MeshLab 2022.02 (Cignoni *et al.*, 2008) was used to generate a 3D surface model and estimate its volume. The volume of the endocast was measured independently via water displacement using a 250 mm graduated cylinder.

SYSTEMATIC PALEONTOLOGY

MAMMALIA Linnaeus, 1758
XENARTHRA Cope, 1889
FOLIVORA Delsuc *et al.*, 2001
MEGATHERIOIDEA Gray, 1821
HAPALOPS Ameghino, 1887

***Hapalops* sp.**

Figures 2–4

Referred material. SGOPV 2077, partial distal phalanx; SGOPV 2113, four postcranial elements including a mostly complete left astragalus, an intermediate phalanx, and a partial glenoid fossa of the scapula; SGOPV 2289, partial molariform tooth; SGOPV 2374, two metapodials; SGOPV 2388, slightly distorted natural endocast lacking olfactory bulbs.

Geographic occurrence. Pampa Castillo, between the Meseta Guadal and Lago General Carrera, Aysén Region, southern Chile (see Flynn *et al.*, 2002b).

Stratigraphic occurrence. Fossil horizons 1 (SGOPV 2388), 5 (SGOPV 2077, SGOPV 2113), 7 (SGOPV 2374), and 8 (SGOPV 2289) of the unnamed formation at Pampa Castillo, Chile; late Early Miocene (Burdigalian/Santacrucian SALMA age).

Comments. Morphology-based phylogenetic analyses have generally found *Hapalops* to be an early-diverging member of the superfamily Megatherioidea (Gaudin, 2004) or a member or close relative or the family Megalonychidae Gervais, 1855 (*e.g.*, Amson *et al.*, 2017; Varela *et al.*, 2019; Casali *et al.*, 2022). However, new collagen and mitochondrial DNA data recovered from more than a dozen Pleistocene sloth species have called into question the compositions of traditionally recognized families (Delsuc *et al.*, 2019; Presslee *et al.*, 2019). A recent phylogenetic study using a Bayesian total-evidence approach with both morphological and molecular data recovered *Hapalops* as a member of Megatherioidea, perhaps closely related to extant three-toed sloths (species of *Bradypus* Linnaeus, 1758), with its position varying depending on the taxa included and the model parameters used (Tejada *et al.*, 2024). There is little doubt that *Hapalops* pertains to the Megatherioidea, but its precise relationships within that clade remain unresolved.

The size and structure of all five Pampa Castillo sloth specimens described herein are compatible with the interpretation that they pertain to a single species. Thus, we conservatively refer them to a single species pending recovery of materials that from this site that would suggest otherwise.

DESCRIPTION

Dental remains

Specimen SGOPV 2289 (Fig. 2.1) is a small portion of the occlusal surface of what presumably was a simple, roughly quadrangular molariform tooth. Along the longest unbroken edge, the cementum layer is beveled, indicating that it represents part of the mesial or distal face (Fig. 2.1, right). The occlusal surfaces of the internal tissue layers (orthodentine externally and vasodentine centrally; Kalthoff, 2011, 2020) are not preserved. The tooth fragment measures 8.25 mm parallel to the longest face, a value within the range of molariform teeth of smaller species of *Hapalops* such as *Hapalops elongatus* Ameghino, 1891c (*e.g.*, Scott, 1903: p. 218).

Postcranial remains

Specimen SGOPV 2077 (Fig. 2.2) is the proximal portion of a laterally compressed ungual (distal) phalanx, probably of the manus considering its relatively gracile proportions. Only small portions of the osseous sheath are preserved.

The specimen measures 11.3 mm in greatest mediolateral breadth on its proximal end and 16.9 mm in greatest dorsopalmar diameter at the base of the bony ungual core. The ungual core itself is narrow, measuring 6.9 mm in width at its base and 3.7 mm at the distalmost end. The articular facet is sub-symmetrical. In lateral view, the dorsal surface of the ungual core is gently convex. In superior view, the ungual core deviates to one side at a slight (~10°) angle.

Specimen SGOPV 2113 includes four elements. One of these is a well-preserved left astragalus missing small portions of bone on the dorsomedial part of the head, the lateral portion of the head and adjacent area of the lateral trochlea, proximolateral part of the lateral trochlea, distal portion of the ectal facet, and the proximomedial part of the ectal facet (Fig. 3.1, 3.7–3.9). The astragalus is 27.4 mm in proximodistal diameter and 24.3 mm across the trochlea. Thus, it is slightly smaller than that of (*i.e.*, within 15% of) *H. elongatus* (31–32 mm; Scott, 1904: p. 231) and

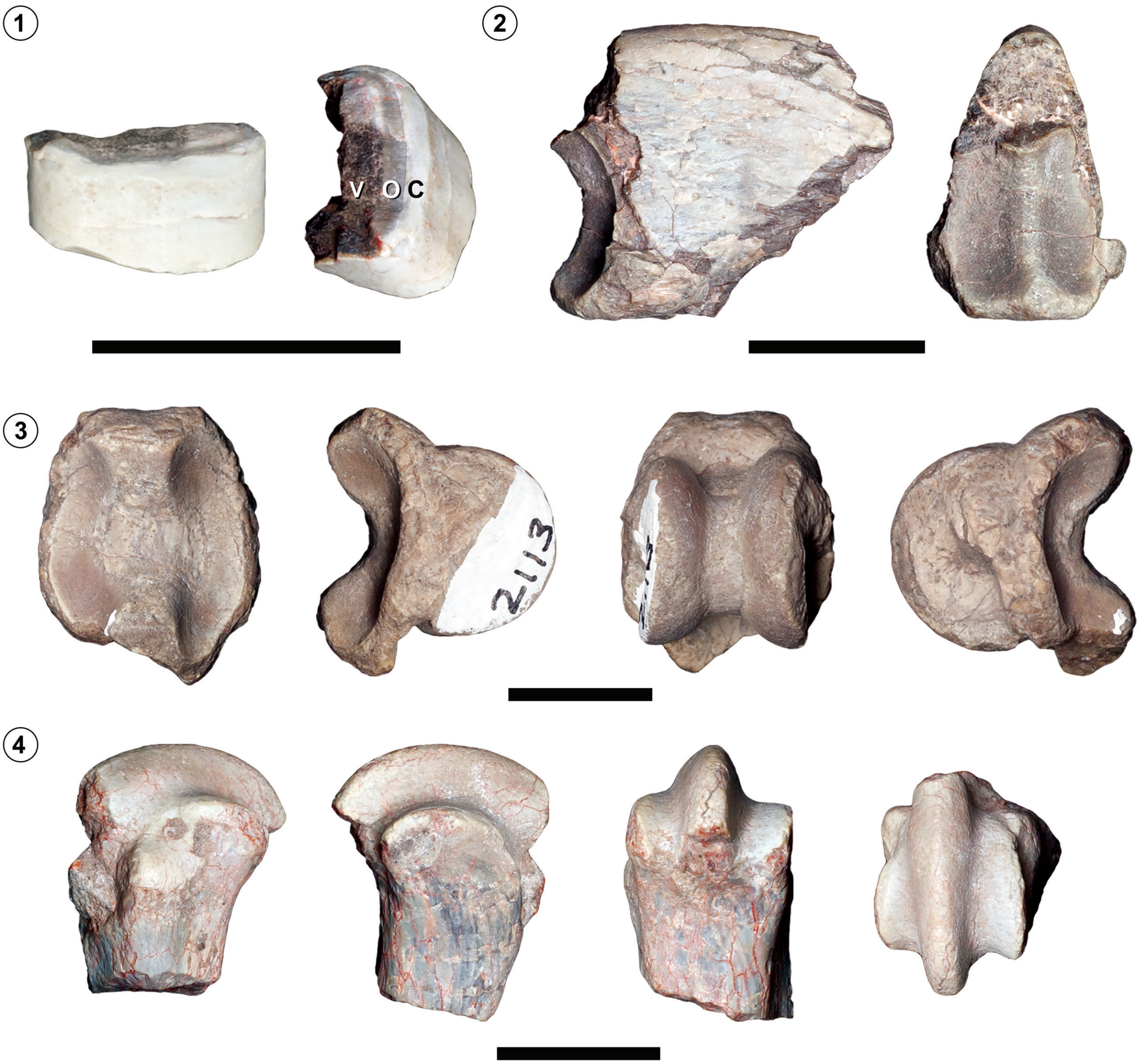

Figure 2. Dental and postcranial specimens referred to ***Hapalops*** sp. from the Santacrucian SALMA-aged Pampa Castillo Fauna, Chile. **1, SGOPV** 2289, partial molariform tooth in mesial or distal (left) and oblique occlusal (right) views. Abbreviations: **C,** cementum; **O,** orthodentine; **V,** vasodentine; **2, SGOPV** 2077, proximal manual? ungual phalanx in mediolateral (left) and proximal (right) views; **3, SGOPV** 2113, intermediate phalanx, probably of pedal digit III, in proximal (left), medial? (center left), distal (center right), and lateral? (right) views; **4, SGOPV** 2374, distal metapodial in lateral? (left), medial? (center left), inferior (center right), and distal (right) views. Scale bars equal 1 cm.

Schismotherium fractum Ameghino, 1887 (31.5 mm; FMNH PM 13137; Fig. 3.2); *ca*. 75–80% the size of *Pelecyodon cristatus* Ameghino, 1891c (33.3 mm; FMNH PM 12062; Fig. 3.6), *Xyophorus atlanticus* Ameghino, 1891c (*ca*. 34 mm; Bargo *et al*., 2019; Fig. 3.3), and *Nematherium* sp. (35 mm; Scott, 1904: p. 351); and *ca*. 65–75% the size of *H. longiceps* (42 mm; Scott, 1903: p. 204; Fig. 3.5) and *Mcdonaldocnus bondesioi* (Scillato-Yané, 1979) (*ca*. 38–42 mm; Gaudin *et al*., 2023: fig. 5).

The largest and most conspicuous feature dorsally on the astragalus of SGOPV 2113 is the lateral trochlea (Fig. 3.1). Its dorsal surface is broad, transversely flat, and of relatively uniform width between its proximal juncture with the medial trochlea and its distal terminus (Fig. 3.9). By contrast, the medial trochlea is broadest distally and narrows toward its proximal confluence with the lateral trochlea. The dorsal surface of the medial trochlea is notably convex proximodistally (Fig. 3.8, upper) but less pronounced than the well-developed odontoid processes of megatheriids (*Planops* Ameghino, 1887; *Prepotherium* Ameghino, 1891a) and mylodontids (*Nematherium* and, presumably, *Analcitherium* Ameghino, 1891c). The angle between the two trochleae is *ca*. 35°, within the range of specimens of *Hapalops* (Gaudin *et al*., 2023) and close to that of *P. cristatus* (36° in FMNH PM 12062; Fig. 3.6); this angle is greater than that of *X. atlanticus* (25°; Bargo *et al*., 2019; Fig. 3.3) and *S. fractum* (21° in FMNH PM 13137; Fig. 3.2) and less than that of most geologically younger sloths (~90°; Gaudin *et al*., 2023). A pronounced pit to accommodate the anterior distal tibial process is present distally, lateral to the juncture of the astragalar neck and body and medial to the distal end of the lateral trochlea. The structure has been described as characteristic of nothrotheriids (Gaudin *et al*., 2023). The width of the astragalar neck cannot be determined because its lateral portion (perhaps 40% of its original breadth) is not preserved. The concave articular facet for the navicular, a synapomorphy of pilosans (Hoffstetter, 1958; Gaudin & McDonald, 2008), is visible in dorsal view due to its slightly dorsal orientation (Fig. 3.1).

On the plantar surface of the astragalus of SGOPV 2113 (Fig. 3.7), the ectal (lateral) facet for articulation with the calcaneum is large and crescentic, as noted by Gaudin *et al.* (2023) for *Hapalops* spp. It measures 10.4 mm at its broadest point, just distal to the midpoint. Its lateral border is less indented than in *P. cristatus* (FMNH PM 12062), *S. fractum* (FMNH PM 13137), and the specimen of *Hapalops* figured by Gaudin *et al.* (2023: fig. 5i); in this regard, it resembles the condition in *M. bondesioi* (Gaudin *et al.,* 2023: fig. 5f) and *Xyophorus* Ameghino, 1887 (Bargo *et al*., 2019: fig. 6.6). The plantar surface of the ectal facet is concave proximodistally but not completely flat mediolaterally; it is canted slightly laterally at its distal end, as Gaudin *et al.* (2023) described for *Hapalops.* The sustentacular (medial) facet for articulation with the calcaneum is small (*ca*. 7.3 x 6.9 mm), subquadrangular, and oriented in a mainly proximal direction (also slightly medial and plantar) rather than a predominantly plantar direction. It is separated from the ectal facet by a narrow sulcus tali (1.6 mm wide), similar to that of *Hapalops* and unlike the condition in *P. cristatus* (FMNH PM 12062), *Schismotherium* Ameghino, 1887 (FMNH PM 13137), *M. bondesioi* (Gaudin *et al*., 2023), and *X. atlanticus* (Bargo *et al*., 2019). The facet for articulation with the cuboid on the plantar surface of the head is larger and more conspicuous than the sustentacular facet. It is smoothly convex along a distomedial-proximolateral axis, and its maximal proximodistal extent is *ca*. 8.3 mm.

The distal morphology of SGOPV 2113 is limited in distal view due to the incomplete preservation of the medial head and neck mentioned previously (Fig. 3.1, 3.9, lower). The navicular facet is notably concave; the preserved portion is subcircular but could have been transversely broad prior to being damaged, as in other early-diverging sloths. Gaudin *et al.* (2023) noted depth/width ratios of 0.71–0.82 for *Xyophorus*, *Pronothrotherium* Ameghino 1907, and specimens of *Hapalops*, in contrast to 0.98 for *M. bondesioi*. The medial condyle of SGOPV 2113 is only slightly taller and much narrower than the lateral condyle in distal view (Fig. 3.9, lower), similar to the condition in *Hapalops* (Gaudin *et al*., 2023) and opposite to the condition in *X. atlanticus* (Bargo *et al*., 2019)

In lateral view (Fig. 3.8, lower), the superior surface of the lateral trochlea is smoothly convex and subtends an arc of *ca*. 125°. The fibular facet is flat, broad distally (at least 11.1 mm), and narrow proximally (*ca*. 2.5 mm based on the portion preserved). Distally, the fibular facet appears to have had relatively broad contact with the ectal facet (this region is incompletely preserved), whereas proximally,

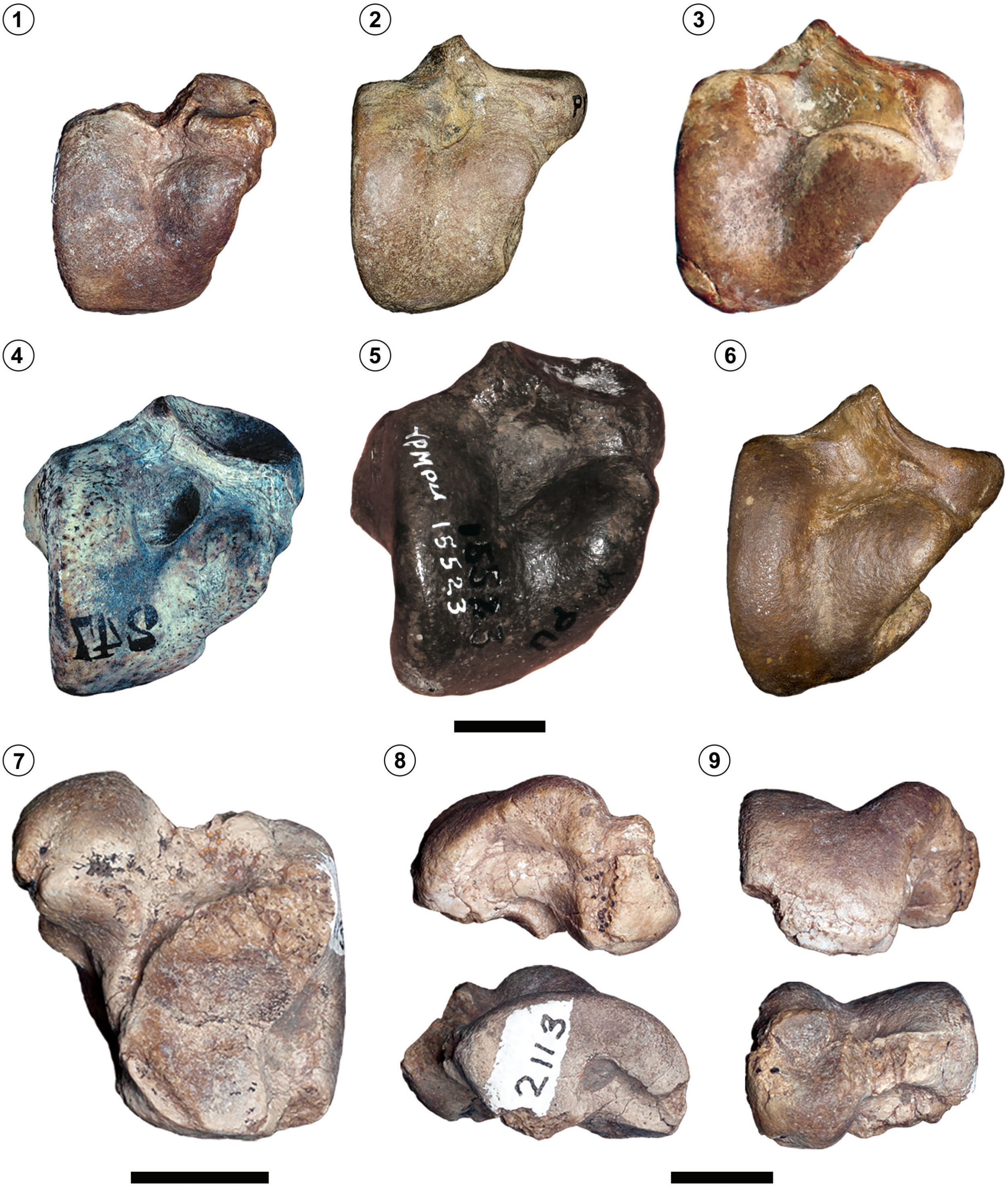

Figure 3. 1–6, Dorsal views of the astragalus of late Early Miocene folivorans. **1,** ***Hapalops*** sp. from the Pampa Castillo Fauna, Chile (**SGOPV** 2113); **2,** ***Schismotherium fractum*** (**FMNH PM** 13137); **3,** ***Xyophorus atlanticus*** (**MPM-PV** 19337; from Bargo *et al.* 2019: fig. 6.5); **4,** ***Hapalops*** sp. (**MLP** 88-X-2-1.4; from Gaudin *et al.* 2023: fig. 5h); **5,** ***Hapalops longiceps*** (**YPM VPPU** 15523); **6,** ***Pelecyodon cristatus*** (FMNH PM 12062). **7–9,** ***Hapalops*** sp. from the Pampa Castillo Fauna, Chile (**SGOPV** 2113); **7,** plantar view; **8,** medial (above) and lateral (below) views; **9,** proximal (above) and distal (below) views. Scale bars equal 1 cm.

the contact appears to have been minimal. This condition is intermediate between that of *Hapalops*, in which the proximal contact is more extensive (Gaudin *et al.*, 2023), and *X. atlanticus*, in which the two facets do not contact one another (Bargo *et al.*, 2019). The latter condition also characterizes *M. bondesioi* (Gaudin *et al.*, 2023: fig. 5f). A deep depression is present inferior to the fibular facet near its midpoint and is still partly filled with matrix (Fig. 3.8, lower).

In medial view (Fig. 3.8, upper), the proximal half of the medial trochlea is essentially flat, whereas the distal half is sharply convex, asymmetrically subtending an angle of *ca*. 90°. The similar dorsoplantar heights of the medial and lateral trochleae resemble the condition in *Hapalops* and other early-diverging sloths and differs from the condition in *M. bondesioi*, in which the lateral trochlea is markedly taller (Gaudin *et al.*, 2023). On the proximal surface of the head, the medial portion of the sustentacular facet is visible and, on the medial surface of the head, a subtriangular, convex facet for articulation with a proximomedial extension of the navicular is present (see Scott, 1903: pl. XXXIII, fig. 4).

The second identifiable element of SGOPV 2113 is a short, broad intermediate phalanx (Fig. 2.3), likely of pedal digit III based on its proportionately large trochlea. Its proximal end is mostly complete, with articular facets that are paired and subequal in size (Fig. 2.3, left). The distal end bears a pronounced trochlea with symmetrical condyles separated by a deep groove that is 2.6 mm in breadth (Fig. 2.3, center right). This phalanx measures 17.5 mm in greatest proximodistal length, 16 mm in greatest mediolateral breadth, and 20 mm in dorsopalmar depth. Other elements of SGOPV 2113 include a small portion of the scapular glenoid and abone fragment of uncertain homology that could represent a vertebral fragment.

Specimen SGOPV 2374 includes two relatively gracile metapodials, each with a pronounced median carina. The shaft of the larger and more complete one (Fig. 2.4) measures 9.05 mm x 8.25 mm (mediolateral x dorsoventral); the corresponding measurement of the smaller one is 6.0 x 6.5 mm. The larger metapodial measures 13.5 mm in greatest dorsoventral height (along the carina); the corresponding portion of the smaller metapodial measures 11.75 mm, but this is a minimum value, as part of the carina is not preserved. These likely correspond to digits IV and V, given that these metapodials are more gracile than those of digits I-III in the manus and pes of *Hapalops* (Scott, 1904, pl. 33, 1904, pl. 41; Toledo *et al.*, 2013: fig. 2m, 2015, fig. 3d).

Natural Endocast

Specimen SGOPV 2388 is a natural endocast lacking the olfactory bulbs. It measures 59.9 mm in greatest length. The specimen is compressed asymmetrically, and the dorsal midline (represented by the superior sagittal sinus) has been displaced *ca.* 15 mm toward the right side relative to the ventral midline (as indicated by the position of the hypophyseal stalk). Thus, in dorsal view, both the dorsal and left lateral surfaces of the endocast are visible (Fig. 4.1). The endocranial volume is 45 cm^3 based on water displacement and 46.17 cm^3 based on a three-dimensional model created from a laser surface scan. However, this is an underestimate of the original volume due to the lack of olfactory bulbs and postmortem distortion. In extant and extinct sloths, the olfactory bulbs account for < 5% of total endocranial volume (Amson *et al.*, 2018; Freitas *et al.*, 2020). Therefore, the original endocast volume was slightly larger, likely closer to 47 or 48 cm^3, although this still represents an underestimate of uncertain magnitude due to the postmortem distortion.

Dorsal surface. The superior sagittal sinus is visible as a pronounced median ridge between the anterior end of the specimen and the junction of the cerebral hemispheres and the cerebellum (Fig. 4.1, 4.3, 4.4, 4.6). A transverse line of bone fragments is present slightly anterior to the anterior-posterior midpoint of the cerebral hemispheres (lower left arrow in Fig. 4.1). Anterior to this line, the sulci and gyri are plainly visible, but posterior to this line, they are overlain by remnants of cerebral vessels and meningeal layers. The transverse line of bone likely represents the position of the frontoparietal suture, with the dura deep to the parietal bone posterior to it. Similar bone remnants are present on the endocast along other presumed suture lines between the parietal and other bones of the cranium, including the occipital posteriorly (upper right arrow in Fig. 4.1) and the squamosal laterally. Dechaseaux (1971) reported vessels preserved on a natural endocast of *Hapalops*, and Dozo (1994) reported them on a natural endocast of *Eucholoeops*.

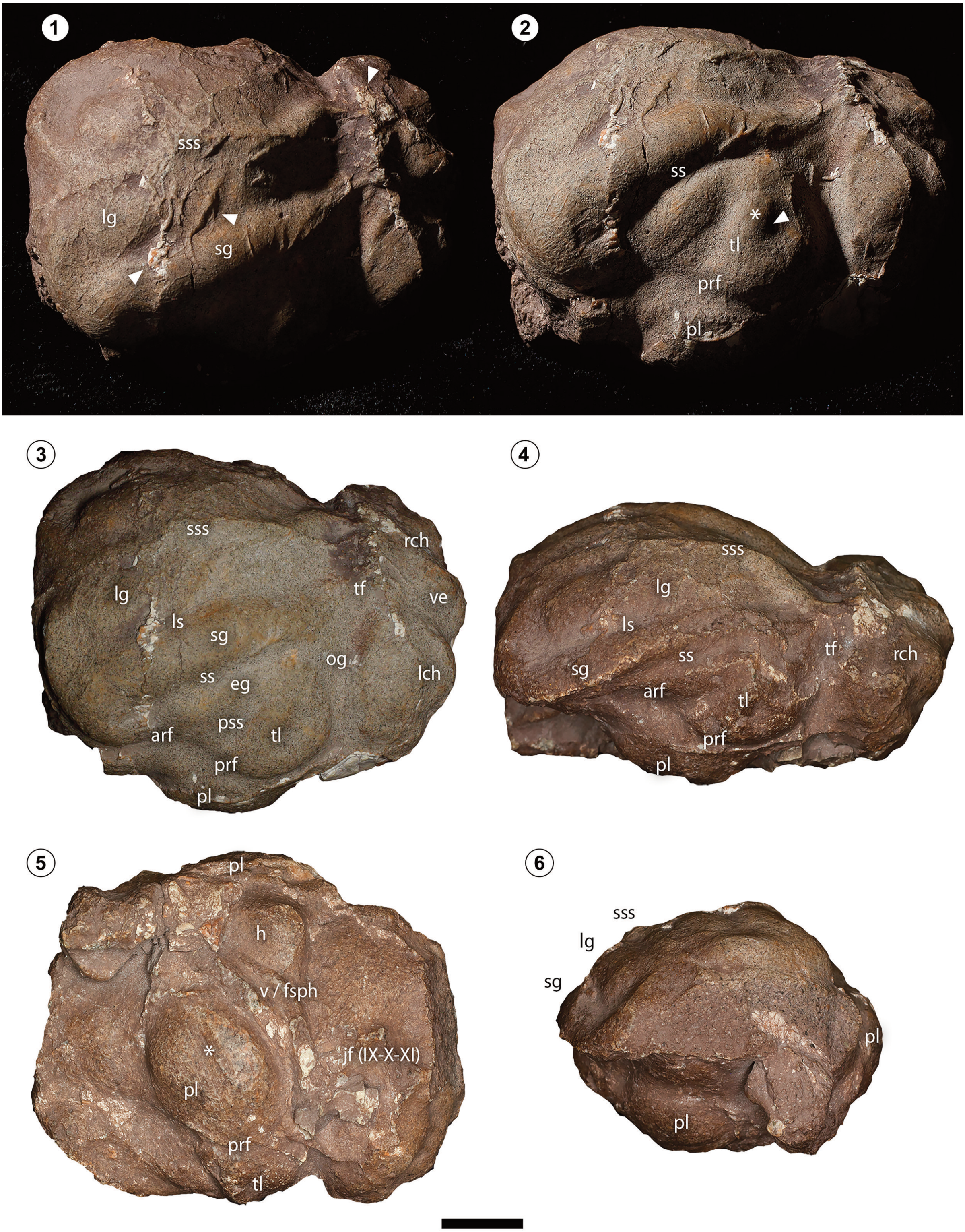

Figure 4. Natural cranial endocast of **SGOPV 2388**, referred to ***Hapalops*** sp., in **1,** dorsal; **2,** left lateral; **3,** dorsal and slightly left lateral; **4,** right lateral (reversed); **5,** ventral; and **6,** anterior views. Oblique lighting accentuating the surface in **1** and **2** with direct lighting in **3–6.** Anterior is toward the left in **1–5**. In **1,** white triangles indicate bony remnants (lower left) and blood vessels (upper left). In **2,** an asterisk marks a rounded elevation of the temporal lobe caudal to the pseudosylvian sulcus, and an arrow marks the sulcus caudal to it. In **5,** an asterisk marks a conspicuous sulcus of uncertain homology. Abbreviations: **arf,** anterior rhinal fissure; **eg,** ectosylvian gyrus; **es,** entolateral sulcus; **h,** hypophysis; **jf,** jugular foramen (egress for cranial nerves IX, X, and XI); **lch,** left cerebellar hemisphere; **lg,** lateral gyrus; **ls,** lateral sulcus; **og,** occipital gyrus; **pl,** pyriform lobe; **prf,** posterior rhinal fissure; **pss,** pseudosylvian sulcus; **rch,** right cerebellar hemisphere; **sg,** suprasylvian gyrus; **ss,** suprasylvian sulcus; **sss,** superior sagittal sinus; **tf,** transverse fissure; **tl,** temporal lobe; **v / fsph,** vessel and/or sphenorbital fissure; **ve,** vermis. Scale bar equals 1 cm.

The suprasylvian gyri demarcate the lateral edges of the dorsal surface of the endocast and diverge slightly anteriorly (Fig. 4.1, 4.3, 4.4). A similar configuration is evident in the endocast of *Hapalops indifferens* described by Dozo (1987). This gyrus is clearer on the left side of SGOPV 2388 than on the right and does not vary appreciably in breadth throughout its length. The lateral sulcus, medial to the suprasylvian gyrus, broadens and bifurcates anteriorly, as described by Dechaseaux (1971) and Dozo (1987). Among other extinct folivorans, a similar bifurcation has only been reported in *Eucholoeops* (Dozo, 1994), also from the late Early Miocene (Santacrucian SALMA) of Patagonia (Scott, 1904). A lateral sulcus that bifurcates anteriorly (Fig. 4.3, 4.4) is also variably present in extant *Bradypus* Linnaeus, 1758. For example, in the extant *Bradypus* specimen studied by Pohlenz-Kleffner (1969, abb. 13), the right lateral sulcus bifurcates anteriorly, but the left does not. Saraiva & Magalhaes-Castro (1975, p. 184) described this sulcus as variable in the specimens they studied ("occasionally subdivided into two separate segments"), and in their schematic drawing, it bifurcates anteriorly (Saraiva & Magalhaes-Castro, 1975: fig. 1). By contrast, the lateral sulcus is simple and non-bifurcating in the *Bradypus* specimen studied by Boscaini *et al.* (2020b).

No enterolateral sulcus is visible in SGOPV 2388, though the details of this region of the endocast are obscured by the presumed dural remnants. The absence of an entolateral sulcus is a presumably ancestral character state in *Hapalops*, *Eucholoeops*, and *Bradypus* (Dozo, 1994; Boscaini *et al.*, 2023). The cerebellum is clearly demarcated from the cerebral hemispheres by a distinct transverse fissure (Fig. 4.1–4) and is similar in breadth to the anterior cerebrum. A vermis is present and well-developed (Fig. 4.3), as in *Choloepus* Linnaeus, 1758, *Glossotherium* Owen, 1839, and *Catonyx* Ameghino, 1891b but unlike in *Bradypus*, where it is absent (Pohlenz-Kleffner, 1969; Boscaini *et al.*, 2020a, 2020b, 2023; Freitas *et al.*, 2020). The vermis is bordered laterally by deep paramedian fissures, as described by Dozo (1987) for *H. indifferens*. Dechaseaux (1971) noted two transverse fissures on the vermis of *Hapalops*, though no transverse fissures were noted for *Hapalops* by Dozo (1987). Dozo (1994) only reported a primary fissure in *Eucholoeops*, and a similar condition appears to be present in SGOPV 2388, though this area is obscured by remnants of the cranial vault, meninges, and blood vessels.

Lateral surface. Features of the lateral surface are more easily seen and interpreted on the left side of the endocast (Fig. 1.2–3), than on the right (Fig. 1.4). The rhinal fissure—split into anterior (arf) and posterior (prf)—is incompletely preserved but is subhorizontal and broadly undulating, as described in *Hapalops* by Dechaseaux (1971) and Dozo (1987). This condition is more like that of *Choloepus* and *Eucholoeops* than *Bradypus*, *Catonyx*, and *Glossotherium*, in which the anterior and posterior portions of the sulcus are strongly angled relative to one another (Dozo, 1994; Boscaini *et al.*, 2020a, 2020b; Freitas *et al.*, 2020). Dozo (1987) noted a sulcus extending superiorly and posteriorly from the rhinal fissure in *Hapalops* and homologized it with the pseudosylvian sulcus. This pseudosylvian sulcus is visible on the left side of SGOPV 2388 (Fig. 4.3) and present in other extant and extinct sloths (Dozo, 1994; Boscaini *et al.*, 2020a, 2020b). In SGOPV 2388, it is oriented at a relatively steep angle to horizontal, a condition more like that of *Hapalops* (Dozo, 1987) than *Eucholoeops* (Dozo, 1994). The temporal lobe of SGOPV 2388 (Fig. 4.2) resembles that of *Bradypus* (Boscaini *et al.*: 2020b, fig. 2k) in having a pronounced rounded elevation caudal to the pseudosylvian sulcus (indicated by an asterisk in Fig. 4.2) that is separated caudally from the remainder of the lobe by a shallow sulcus. Such structures were not mentioned by Dechaseaux (1971) or Dozo (1987) for *Hapalops* or by Dozo (1994) for *Eucholoeops*. However, a sulcus in the region of the temporal lobe, posterior and perpendicular to the pseudosylvian sulcus, was illustrated for *Hapalops* by Dechaseaux (1971: fig. 11). The pyriform lobe of SGOPV 2388 (Fig. 4.2–4) is similar in size to the temporal lobe and positioned slightly more anteriorly, more like the condition in *Bradypus* than *Choloepus* (Boscaini *et al.*, 2020b). These lobes are subequal in size in *Hapalops* (Dozo, 1987), but the temporal lobe is smaller in *Eucholoeops* (Dozo, 1994).

Ventral surface. The most conspicuous structure on the ventral surface of SGOPV 2388 is the right pyriform lobe, which is located near the center of the endocast due to the compression and distortion noted previously (Fig. 4.5). The left pyriform lobe is only visible in profile. A conspicuous groove of uncertain homology traverses the right pyriform lobe caudolaterally to rostromedially (marked by an asterisk in Fig. 4.5). No equivalent sulcus is visible on the left pyriform lobe. The hypophysis is prominent, as in *Choloepus* but unlike in *Bradypus* (Pohlenz-Kleffner, 1969; Boscaini *et al.*, 2020b), and is positioned slightly posterior to the pyriform lobes. The hypophyseal region has not been described for *Hapalops* or *Eucholoeops* (Dechaseaux, 1971; Dozo, 1987, 1994). Between the right pyriform lobe and hypophysis of SGOPV 2388 are grooves and elevations that likely represent the inferior petrosal sinus, internal carotid artery, and/or part of the sphenorbital fissure (Fig. 4.5). The corresponding area on the left side is obscured by bone remnants and matrix, as is the area rostral to the hypophysis. A small protuberance near the caudal end of the right side of the endocast may represent the jugular foramen ("jf (IX-X-XI)" in Fig. 4.5), based on comparisons with extant folivorans (Boscaini *et al.*, 2020b: fig. 2). This area is obscured by bone and matrix on the left side of the specimen. The right temporal lobe is visible posterolateral to the pyriform lobe in ventral view (Fig. 4.5).

Anterior surface. The distortion of the specimen is evident in anterior view (Fig. 4.6); the superior sagittal sinus is positioned *ca.* 45° to the left of vertical, and the right pyriform lobe is on the ventral surface. When the specimen is positioned such that the superior sagittal sinus is in anatomical position, the temporal lobes do not extend laterally beyond the pyriform lobes, in contrast to the condition in *G. robustum*, in which they extend beyond the pyriform lobes (Boscaini *et al.*, 2020b). Rather, they are of similar breadth, as in *Choloepus* and *Bradypus*.

Comments. Overall, the endocast of SGOPV 2388 compares closely with the endocranial cavity of late Early Miocene *Hapalops,* as described and illustrated by Dechaseaux (1971) and Dozo (1987). By contrast, it differs in several respects from that of Early Miocene *Eucholoeops*. Specimen SGOPV 2388 could pertain to a different Early Miocene sloth genus, but this possibility cannot be evaluated without new endocranial data from contemporaneous species.

DISCUSSION

Lack of clarity in the alpha taxonomy of the genus *Hapalops* is a long-standing and well-known issue that remains unresolved (Scott, 1903, 1904; De Iuliis & Pujos, 2006; Bargo *et al.,* 2012, 2019). Mones' (1986) taxonomic compilation of South American vertebrates lists 26 species of *Hapalops*, a number that is far too great considering that most of these species are based on remains from a single geological formation (*i.e.*, the Santa Cruz Formation); a preliminary analysis of craniodental remains from this formation indicated that only four main morphotypes are present (De Iuliis & Pujos, 2006). However, definitive results have yet to be published.

Given the context described above, a specific identification of the *Hapalops* remains from Pampa Castillo would be challenging, even if they were more complete. Nevertheless, the specimens pertain to a relatively small *Hapalops* species, comparable to or slightly smaller than *H. angustipalatus*, *H. elongatus*, and *H. ruetimeyeri* from the Santa Cruz Formation. This is indicated by the length of the astragalus (~15% smaller than *H. elongatus*) as well as the volume of the natural endocast, which is roughly half the size of that of *H. indifferens* (Dozo, 1987), one of the larger Santa Cruz species (along with other large species, *H. longiceps* and *H. platycephalus*). Notably, the difference in endocast volume between SGOPV 2388 and *H. indifferens* (*ca.* 1:2) parallels differences in inferred body mass (BM) between smaller and larger *Hapalops* species; the study of Toledo *et al.* (2014) suggests a BM range of *ca.* 20–40 kg for these smaller species and *ca.* 50–80 kg for larger ones. Thus, 20–40 kg is likely a reasonable BM estimate for *Hapalops* sp. from Pampa Castillo.

Dechaseaux (1971) did not list a species identification for the *Hapalops* specimen she studied (MNHN SCZ 213), and it has not been referred to a species in more recent studies. That cranium measures *ca.* 133 mm from the occipital condyles to the anterior tip of the maxilla based on images of a surface rendering produced from a CT scan (courtesy of G. Billet). This is close to the *H. longiceps* value of 136 mm published by Scott (1903: p. 182) and *ca.* 20% greater than comparable measurements for *H. ruetimeyeri* (Scott 1904: p. 425). Thus, MNHN SCZ 213 appears to pertain to one of the larger Santa Cruz Formation species, making it distinct from the species of *Hapalops* at Pampa Castillo.

The EQ of *Hapalops* sp. from Pampa Castillo is estimated at 0.40 based on an endocranial volume of 47.5 cm^3 (the midpoint of the range estimated for SGOPV 2388 if olfactory bulbs were preserved) and a BM of 30 kg (the midpoint of the range note above; Supplementary Data

S7). This is far below published estimates for extant species of *Bradypus* and *Choloepus* (0.68–0.90 and 0.76–0.87, respectively; Boddy *et al.*, 2012: tab. S1). It is also well below the value of 0.71 published by Dozo (1987) for *H. indifferens*, though its EQ value decreases to 0.58 when a more likely BM of 50 kg is used for that specimen (Supplementary Data S7). The EQ of *Hapalops* sp. from Pampa Castillo is close to that of *E. ingens* (0.48) when the BM of the *Eucholoeops* specimen is estimated at 44 kg based on postcranial measurements and a broad comparative dataset of extant mammals (see Toledo *et al.*, 2014 and "Comparative and analytical methods" above) rather than *ca.* 21.8 kg based on estimated head-body length and a comparative dataset of only extant xenarthrans (Dozo, 1987, 1994). Using this lower BM estimate, Dozo (1994) calculated EQs of 0.77 and 0.67 for *E. ingens* based on equations of Jerison (1973) and Martin (1981), respectively. The more recent equation of Boddy *et al.* (2012) yields an EQ of 0.81 using this lower BM estimate.

The data above suggest an EQ range of *ca.* 0.4–0.6 for Early Miocene megatherioids, a range lower than that of extant sloths (*ca.* 0.7–0.9) but greater than that of large to very large (*ca.* 450–4,600 kg) late Pleistocene sloths. Published EQs for extinct species of the sloths *Catonyx*, *Lestodon*, *Glossotherium*, *Megalonyx*, *Nothrotherium*, and *Paramylodon* range from *ca.* 0.2–0.45 (Tambusso, 2013; Tambusso & Fariña, 2015; Boscaini *et al.*, 2020a), though this range decreases to *ca.* 0.2–0.3 when BM estimates from McDonald (2005) are used for North American species (Supplementary Data S7). If the EQ values for Early Miocene species are close to the ancestral condition for folivorans, this suggests a pattern of parallel increases in EQ in the two genera of extant "tree sloths" and parallel decreases of EQ in larger "ground sloths." Such a pattern could be related to a combination of ecology (especially locomotion) and body size. Exploring this pattern further in a phylogenetic context (*e.g.*, using the phylogenetic encephalization quotient or PEG; Ni *et al.*, 2019; Perini *et al.*, 2022) would be an intriguing line of future research but would require calculating EQ values for additional extinct species, especially those from the late Oligocene, Middle to Late Miocene, and Pliocene.

The original report on the Pampa Castillo Fauna by Flynn *et al.* (2002b) listed a single sloth species at the site. Our review of this collection supports this conclusion and highlights the scarcity of sloth remains at the site; of the more than 650 specimens that have been identified to order, only the five described herein (< 1%) can confidently be assigned to Folivora. This represents a smaller proportion of specimens than for any other major mammal clade at Pampa Castillo, except the hypercarnivorous sparassodonts, which are known from a single specimen and are rare at all South American sites (Croft, 2006; Croft *et al.*, 2018; Engelman *et al.*, 2020).

The scarcity of sloths at Pampa Castillo contrasts dramatically with their abundance in the Santa Cruz Formation (*e.g.*, Scott, 1903; Bargo *et al.*, 2019), where they typically account for ~8–10% or more of identified specimens (Croft, 2013, app. 1; Cuitiño *et al.*, 2019; Kay *et al.*, 2021). By contrast, sloths are even less common in the nearby Pinturas Formation than at Pampa Castillo, at least as indicated by the number of published specimens. Brandoni *et al.* (2016) described only three sloth specimens from the very large sample of Pinturas Formation fossils collected in the 1980s by teams from the Museo Argentina de Ciencias Naturales (Buenos Aires) and the State University of New York at Stony Brook. More than 400 rodent specimens are present in the same collections (Kramarz & Bellosi, 2005), in addition to dozens of specimens of primates (Fleagle *et al.*, 1987; Fleagle, 1990; Tejedor, 2002) and palaeothentoid marsupials (Bown & Fleagle, 1993). The ratio of sloth to litoptern specimens likely yields a more accurate quantitative comparison between Pampa Castillo and Pinturas, as litopterns are more similar to Early Miocene sloths in terms of body size and diet than are rodents, primates, and palaeothentoids. This ratio is 1:3.2 at Pampa Castillo (five sloth specimens in our study and 16 litoptern specimens from McGrath *et al.*, 2020) versus 1:55 for Pinturas (three sloth specimens from Brandoni *et al.*, 2016, and 165 litoptern specimens from Kramarz & Bond, 2005). By contrast, sloths are slightly more abundant than litopterns in the Santa Cruz Formation (*ca.* 0.55–0.85 litoptern specimens per sloth specimen; Croft, 2013, app. 1; Cuitiño *et al.*, 2019; Kay *et al.*, 2021).

Despite the small number of sloth specimens described from the Pinturas Formation, at least two species are represented (*Hapalops* sp. and *Schismotherium* cf. *S. binum*; Brandoni *et al.*, 2016), and two others may even be present in the formation (*i.e.*, *Pelecyodon arcuatus* and *Proprepotherium deseadense* have been described for the “fauna Astrapothericulense” but may or may not be from the Pinturas Fm.; Brandoni *et al.*, 2016). All these occurrences in the Pinturas Formation are poorly characterized (Brandoni *et al.*, 2016; see also Carlini *et al.*, 2013), but the *Hapalops* sp. from Pampa Castillo seems to be slightly smaller than the *Hapalops* species of the Pinturas Formation (which may pertain to *H. curvus*; Brandoni *et al.*, 2016). However, a lack of comparable elements precludes precise quantitative comparisons. Pampa Castillo rodent species are more similar to those of coastal Santa Cruz Formation sites than Pinturas Formation sites (McGrath *et al.*, 2023), so ultimate referral of the Pampa Castillo *Hapalops* to a small-bodied Santa Cruz Formation species rather than *H. curvus* would not be unexpected.

The site of Sierra Baguales in southern Chile is similar in age to Pampa Castillo, and the abundance of sloth remains is comparable. Bostelmann *et al.* (2013) mentioned only three sloth specimens of more than 200 vertebrate specimens collected, and Bostelmann and Oyarzún (2013) reported a fourth specimen, a total representing < 2%. These fragmentary remains pertain to two species, the smaller of which has affinities with *Pelecyodon* and *Hapalops* (Bostelmann & Oyarzún, 2013). Given the similar age, size, and broad taxonomic affinities, it is possible that this smaller Sierra Baguales species is the same one represented at Pampa Castillo.

At present, the only well-defined Early Miocene sloth species from southern Chile is the mylodontid *Nematherium birdi*, which is based on a partial cranium from the Palomares Formation (Simpson, 1941). This genus has yet to be recorded from the Pinturas Formation, but Kramarz *et al.* (2010) referred a partial right dentary from ‘Pinturan’ levels at Gran Barranca (Chubut, Argentina) to *Nematherium* sp. The genus has also been documented in late Early Miocene (Burdigalian/Santacrucian) levels of Estero Correntoso at Laguna del Laja in south-central Chile (considered to be *Nematherium* cf. *N. angulatum* or sp. nov.; Flynn *et al.*, 2008). Thus, *Nematherium* was relatively widespread during this time interval. What is unclear is whether the presence and/or abundance of *Nematherium* at these sites reflects local climate/habitat differences relative to sites where mylodontids such as *Nematherium* have yet to be sampled (*e.g.*, Pampa Castillo and Sierra Baguales) or sites where they are vastly outnumbered by megatherioids (*e.g.*, the Santa Cruz Formation; Scott, 1903, 1904; Croft, 2013; Bargo *et al.*, 2012, 2019; Cuitiño *et al.*, 2019; Kay *et al.*, 2021).

The high abundance of sloths in the Santa Cruz Formation distinguishes it from virtually all other late Early Miocene sites in southern South America. It is also a notable point of contrast with the Chucal Fauna in northernmost Chile (~18.75° S; Arica and Parinacota regions; Flynn *et al.*, 2002a). More than 220 specimens have been collected from this site thus far, excluding the many small mammal remains collected from the well-indurated green sandstones, mudstones, and limestones of Member W3 (see Croft *et al.*, 2021), and sloth remains have yet to be identified there (Croft *et al.*, 2004, 2007). This suggests that sloths were relatively uncommon at Chucal, at least compared to other medium to large herbivores, similar to the pattern at other Early Miocene sites in Chile.

CONCLUSIONS

All sloth (Folivora/Phyllophaga) remains recovered thus far from the late Early Miocene (Burdigalian; Santacrucian SALMA) site of Pampa Castillo in southern Chile pertain to a single, relatively small-bodied species of *Hapalops* (likely 20–40 kg body mass), possibly one of the several small-bodied species documented in the Santa Cruz Formation of southern Argentina. This generic identification is primarily based on the morphology of the astragalus and a natural endocast of the cranial cavity. Other remains referred to this species include fragmentary postcranial bones (phalanges, metapodials, scapula, perhaps a partial vertebra) and a partial molariform tooth. The EQ of *Hapalops* sp. from Pampa Castillo is estimated at 0.40, comparable to that of contemporaneous species (*Hapalops indifferens*, *Eucholoeops ingens*), lower than that of extant tree sloths, and higher than that of late Pleistocene ground sloths. The scarcity of sloth specimens at Pampa Castillo is typical of many late Early Miocene sites from southern South America and contrasts with the unusually high abundance of sloth specimens in the Santa Cruz Formation. This overall pattern invites consideration of the degree to which: 1) Santa Cruz faunas are representative of approximately contemporaneous faunas elsewhere in South America; and 2) taphonomic processes, local climate/vegetation, and biogeography contribute to observed differences in taxonomic diversity and abundance among these late Early Miocene sites.

ACKNOWLEDGMENTS

This manuscript is modified from Nathanael Lee's senior Capstone paper, submitted in partial fulfillment of the Bachelor of Science in Biology degree at Case Western Reserve University. We thank A. Boscaini for providing the digital models of the cranial endocasts for *Glossotherium*, *Choloepus*, and *Bradypus*; G. Billet for providing images of MNHN SCZ 213; T. Gaudin for providing photos of YPM VPPU 15523; A. Boscaini and G. De Iuliis for providing thoughtful critical reviews that improved the final version of this manuscript; and P. Olivier-Antoine for taking editorial responsibility of the manuscript on behalf of *Ameghiniana*. We are grateful for the continued support and collaboration of our colleague and friend Reynaldo Charrier (Universidad de Chile and Universidad Andres Bello), the directors and staff of the Museo Nacional de Historia Natural, and the Consejo de Monumentos Nacionales, Santiago, Chile, throughout our research on the vertebrate paleontology and geology of Chile. We also appreciate the contributions of our longtime collaborator and friend Daniel Frassinetti (deceased; former Jefe, Area Paleontología, Museo Nacional de Historia Natural, Chile), Greg Buckley, René Burgos, Roger Carpenter, Mark Norell, Michael Novacek, Paul Raty, Paul Sereno, Carlos de Smet, Cruz Vargas, and members and friends of the de Smet family for participating in and/or assisting with fieldwork at Pampa Castillo, which was supported financially by the Eppley Foundation for Scientific Research and the American Museum of Natural History.

REFERENCES

Abello, M. A., Candela, A. M., & Ortiz-Jaureguizar, E. (2012). Paleoecology of the Paucituberculata and Microbiotheria (Mammalia, Marsupialia) from the late Early Miocene of Patagonia. In M. S. Bargo, R. F. Kay, & S. F. Vizcaíno (Eds.), *Early Miocene Paleobiology in Patagonia: High-Latitude Paleocommunities of the Santa Cruz Formation* (pp. 156–172). Cambridge University Press.

Ameghino, F. (1887). Enumeración sistemática de las espécies de mamíferos fósiles coleccionados por Carlos Ameghino en los terrenos Eocenos de la Patagonia austral y depositados en el Museo de La Plata. *Boletín del Museo La Plata*, *1*, 1–26.

Ameghino, F. (1891a). Enumeration synoptique des especes de mammifères fossiles des formations éocènes de Patagonie. *Boletin de la Academia Nacional de Ciencias en Cordoba, 13*, 259–452.

Ameghino, F. (1891b). Mamíferos y aves fósiles Argentinos: espécies nuevas: adiciones y correcciones. *Revista Argentina de Historia Natural*, *1*, 240–259.

Ameghino, F. (1891c). Nuevos restos de mamíferos fósiles descubiertos por Carlos Ameghino en el Eoceno inferior de la Patagonia austral. – Especies nuevas, adiciones y correcciones. *Revista Argentina de Historia Natural*, *1*, 289–328.

Ameghino, F. (1907). Notas sobre una pequeña colección de huesosde mamíferos procedentes de las grutas calcáreas de Iporangaen el estado de São Paulo, Brazil. *Revista do Museu Paulista*, *7*, 59–124.

Amson, E., Billet, G., & Muizon, C. de. (2018). Evolutionary adaptation to aquatic lifestyle in extinct sloths can lead to systemic alteration of bone structure. *Proceedings of the Royal Society B: Biological Sciences*, *285*, 20180270

Amson, E., Muizon, C. de, & Gaudin, T. (2017). A reappraisal of the phylogeny of the Megatheria (Mammalia: Tardigrada), with an emphasis on the relationships of the Thalassocninae, the marine sloths. *Zoological Journal of the Linnean Society*, *179*(1), 217–236.

Bargo, M. S., De Iuliis, G., & Toledo, N. (2019). Early Miocene sloths (Xenarthra, Folivora) from the Río Santa Cruz valley (southern Patagonia, Argentina). Ameghino, 1887 revisited. *Publicación Electrónica de la Asociación Paleontológica Argentina*, *19*(2), 102–137.

Bargo, M. S., Toledo, N., & Vizcaíno, S. F. (2012). Paleobiology of the Santacrucian sloths and anteaters (Xenarthra, Pilosa). In S. F. Vizcaíno, R. Kay, & M. S. Bargo (Eds.), *Early Miocene Paleobiology in Patagonia: High-Latitude Paleocommunities of the Santa Cruz Formation* (pp. 216–242). Cambridge University Press.

Boddy, A. M., McGowen, M. R., Sherwood, C. C., Grossman, L. I., Goodman, M., & Wildman, D. E. (2012). Comparative analysis of encephalization in mammals reveals relaxed constraints on anthropoid primate and cetacean brain scaling. *Journal of Evolutionary Biology*, *25*(5), 981–994.

Bondesio, P., Rabassa, J., Pascual, R., Vucetich, M. G., & Scillato-Yané, G. J. (1980). La formación Collón-Curá del Pilcaniyeu Viejo y sus alrededores (Río Negro, República Argentina). Su antiguedad y las condiciones ambientales según su distribución, su litogénesis sus vertebrados. *Actas del Segundo Congreso Argentino de Paleontología y Bioestratigrafía y Primer Congreso Latinoamerica de Paleontología*, *3*, 85–99.

Boscaini, A., Iurino, D., Sardella, R., Gaudin, T., & Pujos, F. (2023). The endocranial cavities of sloths (Xenarthra, Folivora): Insights from the brain endocast, bony labyrinth, and cranial sinuses. In M. Dozo, A. Paulina-Carabajal, T. Macrini, & S. Walsh (Eds.), *Paleoneurology of Amniotes* (pp. 737–760). Springer.

Boscaini, A., Iurino, D. A., Mamani Quispe, B., Andrade Flores, R., Sardella, R., Pujos, F., & Gaudin, T. J. (2020a). Cranial anatomy and paleoneurology of the extinct sloth *Catonyx tarijensis* (Xenarthra, Mylodontidae) from the Late Pleistocene of Oruro, southwestern Bolivia. *Frontiers in Ecology and Evolution*, *8*, 69.

Boscaini, A., Iurino, D. A., Sardella, R., Tirao, G., Gaudin, T. J., & Pujos, F. (2020b). Digital cranial endocasts of the extinct sloth *Glossotherium robustum* (Xenarthra, Mylodontidae) from the Late Pleistocene of Argentina: description and comparison with the extant sloths. *Journal of Mammalian Evolution*, *27*(1), 55–71.

Bostelmann, J. E., Castro, N., Moreno, K., Garcia, M., Fosdick, J., Campos-Medina, J., Croft, D. A., & Montoya-Sanhueza, G. (2018). *Stratigraphy and paleontology of Caragua, Arica and Parinacota regions, Chile, part 2: biostratigraphy and geochronology of the late Miocene sedimentary sequence.* XV Congreso Geológico Chileno (p. 1321). Concepción.

Bostelmann, J. E., Le Roux, J. P., Vásquez, A., Gutiérrez, N. M., Oyarzún, J. L., Carreño, C., Torres, T., Otero, R., Llanos, A., Fanning, C. M., & Hervé, F. (2013). Burdigalian deposits of the Santa Cruz Formation in the Sierra Baguales, Austral (Magallanes) Basin: Age, depositional environment and vertebrate fossils. *Andean Geology*, *40*(3), 458–489.

Bostelmann, J. E., & Oyarzún, J. L. (2013). Fossil Xenarthra of the Early

Miocene Santa Cruz Formation of Sierra Baguales, Magallanes, Chile: Diversity and biogeographic affinities. *Bollettino di Geofisica*, *54*(Supp. 2), 319–322.

Bown, T. M., & Fleagle, J. G. (1993). Systematics, biostratigraphy, and dental evolution of the Palaeothentidae, later Oligocene to Early–Middle Miocene (Deseadan–Santacrucian) caenolestoid marsupials of South America. *Journal of Paleontology*, *67*(S29), 1–76.

Brandoni, D., Ruiz, L. G., Tejedor, M. F., Martin, G., & Fleagle, J. G. (2016). Megatherioidea (Mammalia, Xenarthra, Tardigrada) from the Pinturas Formation (Early Miocene), Santa Cruz Province (Argentina) and their chronological implications. *Paläontologische Zeitschrift*, *90*(3), 619–628.

Candela, A. M., Rasia, L. L., & Pérez, M. E. (2012). Paleobiology of Santacrucian caviomorph rodents: a morphofunctional approach. In M. S. Bargo, R. F. Kay, & S. F. Vizcaíno (Eds.), *Early Miocene Paleobiology in Patagonia: High-Latitude Paleocommunities of the Santa Cruz Formation* (pp. 287–305). Cambridge University Press.

Campos-Medina, J., Montoya-Sanhueza, G., Moreno, K., Bostelmann, E., & García, M. (2023). Paleohistology of *Caraguatypotherium munozi* (Mammalia, Notoungulata, Mesotheriidae) from the early late Miocene of northern Chile: A preliminary ontogenetic approach. *PLoS ONE*, *18*(3), e0273127.

Canto, J., Salas-Gismondi, R., Cozzuol, M., & Yáñez, J. (2008). The aquatic sloth *Thalassocnus* (Mammalia, Xenarthra] from the late Miocene of north-central Chile: biogeographic and ecological implications. *Journal of Vertebrate Paleontology*, *28*(3), 918–922.

Carlini, A. A., Brandoni, D., & Dal Molin, C. N. (2013). A new genus and species of Planopinae (Xenarthra: Tardigrada) from the Miocene of Santa Cruz Province, Argentina. *Zootaxa*, *3694*, 565–578.

Casali, D. M., Boscaini, A., Gaudin, T. J., & Perini, F. A. (2022). Reassessing the phylogeny and divergence times of sloths (Mammalia: Pilosa: Folivora), exploring alternative morphological partitioning and dating models. *Zoological Journal of the Linnean Society*, *196*(4), 1505–1551.

Cifelli, R., & Soria, M. (1983). Systematics of the Adianthidae (Litopterna, Mammalia). *American Museum Novitates*, *2771*, 1–25.

Cignoni, P., Callieri, M., Corsini, M., Dellepiane, M., Ganovelli, F., & Ranzuglia, G. (2008). MeshLab: an open-source mesh processing tool. *Sixth Eurographics Italian Chapter Conference*, 129–136.

Cope, E. D. (1889). The Edentata of North America. *The American Naturalist*, *23*(272), 657–664.

Croft, D. A. (2006). Do marsupials make good predators? Insights from predator–prey diversity ratios. *Evolutionary Ecology Research*, *8*, 1193–1214.

Croft, D. A. (2013). What constitutes a fossil mammal community in the Early Miocene Santa Cruz Formation? *Journal of Vertebrate Paleontology*, *33*(2), 401–409.

Croft, D. A., Flynn, J. J., & Wyss, A. R. (2004). Notoungulata and Litopterna of the Early Miocene Chucal Fauna, northern Chile. *Fieldiana: Geology (New Series)*, *50*, 1–49.

Croft, D. A., Flynn, J. J., & Wyss, A. R. (2007). A new basal glyptodontid and other Xenarthra of the early Miocene Chucal Fauna, Northern Chile. *Journal of Vertebrate Paleontology, 27*(4), 781–797.

Croft, D. A., Flynn, J. J., & Wyss, A. R. (2008). The Tinguiririca Fauna of Chile and the early stages of "modernization" of South American mammal faunas. *Arquivos do Museu Nacional, Rio de Janeiro*, *66*, 191–211.

Croft, D. A., Engelman, R., Dolgushina, T., & Wesley, G. (2018). Diversity and disparity of sparassodonts (Metatheria) reveal non-analogue nature of ancient South American mammalian carnivore guilds. *Proceedings of the Royal Society B: Biological Sciences*, *285*(1870), 20172012.

Croft, D. A., Flynn, J. J., Wyss, A. R., Charrier, R., & Anaya, F. (2021). New chinchillid rodents (Hystricognathi: Caviomorpha) from northern Chile and Bolivia fill a 17-million-year gap in the pan-chinchilline fossil record. *Journal of Mammalian Evolution 28*(4), 1205–1236.

Croft, D. A. (2016). *Horned armadillos and rafting monkeys: the fascinating fossil mammals of South America.* Indiana University Press.

Cuitiño, J. I., Vizcaíno, S. F., Bargo, M. S., & Aramendía, I. (2019). Sedimentology and fossil vertebrates of the Santa Cruz Formation (Early Miocene) in Lago Posadas, southwestern Patagonia, Argentina. *Andean Geology 46*(2), 383–420.

Dechaseaux, C. (1958). Encéphale de Xénarthres fossiles. In J. Piveteau (Ed.), *Traité de Paléontologie, Tome VI, Volume 2* (pp. 637–640). Maison et Cie.

Dechaseaux, C. (1971). *Oreomylodon wegneri*, édenté gravigrade du Pléistocène de l'Équateur - Crâne et moulage endocrânien. *Annales de Paléontologie*, *57*(2), 243–285.

De Iuliis, G., Bargo, M. S., Toledo, N., Tsuji, L., & Vizcaíno, S. F. (2024). The status of *Eucholoeops fronto* and *E. lafonei* (Xenarthra, Folivora, Megalonychidae) in the systematics of the Early Miocene *Eucholoeops* (Santa Cruz, Argentina). *Ameghiniana*, *61*(1), 45–69.

De Iuliis, G., & Pujos, F. (2006). On the systematics of *Hapalops* (Xenarthra: Megatherioidea). *Journal of Vertebrate Paleontology*, *26*(3 Supp.), 55A.

De Los Arcos, S., Partarrieu, D., Carrillo-Briceño, J., & Amson, E. (2017). The Southernmost Occurrence of the Aquatic Sloth Thalassocnus (Mammalia, Tardigrada) in Two New Pliocene Localities in Chile. *Ameghiniana*, *54*(4), 351–369.

Delsuc, F., Catzeflis, F. M., Stanhope, M. J., & Douzery, E. J. P. (2001). The evolution of armadillos, anteaters and sloths depicted by nuclear and mitochondrial phylogenies: implications for the status of the enigmatic fossil *Eurotamandua. Proceedings of the Royal Society of London B: Biological Sciences*, *268*, 1605–1615.

Delsuc, F., Kuch, M., Gibb, G. C., Karpinski, E., Hackenberger, D., Szpak, P., Martínez, J. G., Mead, J. I., Mcdonald, H. G., Macphee, R. D. E., Billet, G., Hautier, L., & Poinar, H. N. (2019). Ancient mitogenomes reveal the evolutionary history and biogeography of sloths. *Current Biology*, *29*(12), 2031–2042.e6.

Dozo, M. T. (1987). The endocranial cast of an Early Miocene edentate, *Hapalops indifferens* Ameghino (Mammalia, Edentata, Tardigrada, Megatheriidae). Comparative study with brains of recent sloths. *Journal für Hirnforschung*, *28*(4), 397–406.

Dozo, M. T. (1994). Interpretación del molde endocraneano de *Eucholoeops fronto*, un Megalonychidae (Mammalia, Xenarthra, Tardigrada) del Mioceno temprano de Patagonia (Argentina). *Ameghiniana*, *31*(4), 317–329.

Dozo, M. T., Paulina-Carabajal, A., Macrini, T. E., & Walsh, S. (2023). *Paleoneurology of amniotes* (1 ed.). Springer.

Encinas, A., Folguera, A., Riffo, R., Molina, P., Fernández Paz, L., Litvak, V. D., Colwyn, D. A., Valencia, V. A., & Carrasco, M. (2019). Cenozoic basin evolution of the Central Patagonian Andes: Evidence from geochronology, stratigraphy, and geochemistry. *Geoscience Frontiers*, *10*(3), 1139–1165.

Engelman, R. K., Anaya, F., & Croft, D. A. (2020). *Australogale leptognathus*, gen. et sp. nov., a second species of small sparassodont (Mammalia: Metatheria) from the Middle Miocene locality of Quebrada Honda, Bolivia. *Journal of Mammalian Evolution,* 27, 37–54.

Ercoli, M., Prevosti, J., & Forasiepi, A. (2014). The structure of the mammalian predator guild in the Santa Cruz Formation (late

Early Miocene). *Journal of Mammalian Evolution*, *21*, 369–381.

Ferreira, J. D., Negri, F. R., Sánchez-Villagra, M. R., & Kerber, L. (2020). Small within the largest: brain size and anatomy of the extinct *Neoepiblema acreensis*, a giant rodent from the Neotropics. *Biology Letters*, *16*(2), 20190914.

Fleagle, J. G. (1990). New fossil platyrrhines from the Pinturas Formation, southern Argentina. *Journal of Human Evolution*, *19*(1–2), 61–85.

Fleagle, J. G., Perkins, M. E., Heizler, M. T., Nash, B., Bown, T. M., Tauber, A. A., Dozo, M. T., & Tejedor, M. F. (2012). Absolute and relative ages of fossil localities in the Santa Cruz and Pinturas formations. In M. S. Bargo, R. F. Kay, & S. F. Vizcaíno (Eds.), *Early Miocene Paleobiology in Patagonia: High-Latitude Paleocommunities of the Santa Cruz Formation* (pp. 41–58). Cambridge University Press.

Fleagle, J. G., Powers, D., Conroy, G., & Watters, J. (1987). New fossil platyrrhines from Santa Cruz Province, Argentina. *Folia Primatologica*, *48*, 65–77.

Flynn, J. J., Charrier, R., Croft, D. A., Gans, P. B., Herriott, T. M., Wertheim, J. A., & Wyss, A. R. (2008). Chronologic implications of new Miocene mammals from the Cura-Mallín and Trapa Trapa formations, Laguna del Laja area, south central Chile. *Journal of South American Earth Sciences*, *26*, 412–423.

Flynn, J. J., Charrier, R., Croft, D. A., & Wyss, A. R. (2012). Cenozoic Andean faunas: shedding new light on South American mammal evolution, biogeography, environments, and tectonics. In B. D. Patterson & L. P. Costa (Eds.), *Bones, Clones, and Biomes. The History and Geography of Recent Neotropical Mammals* (pp. 51–75). University of Chicago Press.

Flynn, J. J., Croft, D. A., Charrier, R., Gérard, H., & Wyss, A. R. (2002a). The first Cenozoic mammal fauna from the Chilean Altiplano. *Journal of Vertebrate Paleontology*, *22*(1), 200–206.

Flynn, J. J., Croft, D. A., Charrier, R., Wyss, A. R., Hérail, G., & García, M. (2005). New Mesotheriidae (Mammalia, Notoungulata, Typotheria), geochronology and tectonics of the Caragua area, northernmost Chile. *Journal of South American Earth Sciences*, *19*(1), 55–74.

Flynn, J. J., Novacek, M. J., Dodson, H. E., Frassinetti, D., McKenna, M. C., Norell, M. A., Sears, K. E., Swisher, C. C., & Wyss, A. R. (2002b). A new fossil mammal assemblage from the southern Chilean Andes: implications for geology, geochronology, and tectonics. *Journal of South American Earth Sciences*, *15*(3), 285–302.

Flynn, J. J., & Swisher, C. C., III. (1995). Cenozoic South American Land Mammal Ages: correlation to global geochronologies. In W. A. Berggren, D. V. Kent, M.-P. Aubry, & J. Hardenbol (Eds.), *Geochronology, Time Scales and Global Stratigraphic Correlation* (pp. 317–333). Society for Sedimentary Geology.

Flynn, J. J., Wyss, A. R., Croft, D. A., & Charrier, R. (2003). The Tinguiririca Fauna, Chile: biochronology, paleoecology, biogeography, and a new earliest Oligocene South American Land Mammal 'Age'. *Palaeogeography, Palaeoclimatology, Palaeoecology*, *195*(3), 229–259.

Folguera, A., Encinas, A., Echaurren, A., Gianni, G., Orts, D., Valencia, V., & Carrasco, G. (2018). Constraints on the Neogene growth of the central Patagonian Andes at the latitude of the Chile triple junction (45–47°S) using U/Pb geochronology in synorogenic strata. *Tectonophysics*, *744*, 134–154.

Freitas, L. M., Dos Santos, O. P., Santos, A. L. Q., de Melo, F. R., Silveira, L., Jacomo, A. T. A., Pereira, K. F., & Lima, F. C. (2020). Brain anatomy of two-toed sloth (*Choloepus didactylus*, Linnaeus, 1758): A comparative gross anatomical study of extant xenarthrans. *Anatomia, Histologia, Embryologia*, *49*(1), 130–143.

Gaillard, C., Tarquini, S., Hernández Del Pino, S., Ladevèze, S., & Forasiepi, A. (2019). 3D digital endocast of the Early Miocene (Colhuehuapian) *Sipalocyon externa* (Metatheria, Sparassodonta). *Libro de Resúmenes, Reunión de Comunicaciones de la Asociación Paleontológica Argentina* (p. 116). La Plata.

Gaudin, T. J. (2004). Phylogenetic relationships among sloths (Mammalia, Xenarthra, Tardigrada): the craniodental evidence. *Zoological Journal of the Linnean Society*, *140*(2), 255–305.

Gaudin, T. J., Boscaini, A., Mamani Quispe, B., Andrade Flores, R., Fernández-Monescillo, M., Marivaux, L., Antoine, P.-O., Münch, P., & Pujos, F. (2023). Recognition of a new nothrotheriid genus (Mammalia, Folivora) from the early late Miocene of Achiri (Bolivia) and the taxonomic status of the genus *Xyophorus*. *Historical Biology*, *35*(6), 1041–1051.

Gaudin, T. J., & Croft, D. A. (2015). Paleogene Xenarthra and the evolution of South American mammals. *Journal of Mammalogy*, *96*(4), 622–634.

Gaudin, T. J., & McDonald, H. G. (2008). Morphology-based investigations of the phylogenetic relationships among extant and fossil xenarthrans. In S. F. Vizcaíno & W. J. Loughry (Eds.), *The biology of the Xenarthra* (pp. 24–36). University of Florida Press.

Gervais, P. (1855). *Recherches sur les mammifères fossiles de l'amérique méridionale: Mémoire accompagne de dix planches lithographiees.* Forgotten Books, London.

Gervais, P. (1869). Mémoire sur les formes cérébrales propres aux édentés vivants et fossiles. *Nouvelles archives du Muséum d'histoire naturelle*, *5*, 1–56.

Gompertz, R. H. (1902). Specific gravity of the brain. *The Journal of Physiology*, *27*(6), 459–462.

Gray, J. E. (1821). On the natural arrangement of vertebrose animals. *London Medical Repository*, *15*(1), 296–310.

Hernández Del Pino, S., Fernández, M., Cerdeño, E., & Fernicola, J. C. (2019). Anatomy and systematics of *Notohippus toxodontoides* Ameghino, 1891 (Mammalia, Notoungulata), from the Miocene of Santa Cruz Province, Argentina. *Journal of Vertebrate Paleontology*, *39*(1), e1577870.

Hoffstetter, R. (1958). Xenarthra. In J. Piveteau (Ed.), *Traité de Paléontologie, Tome VI, Volume 2* (pp. 535–636). Maison et Cie.

Hoffstetter, R. (1961). Description d'un squelette de *Planops* (gravigrade du Miocène de Patagonie). *Mammalia*, *25*, 57–96.

Jakob, C., & Onelli, C. (1913). *Atlas del cerebro de los mamíferos de la República Argentina. Estudios anatómicos, histológicos y biológicos comparados sobre la evolución de los hemisferios y de la corteza cerebral.* Imprenta de Guillermo Kraft, Buenos Aires.

Jerison, H. J. (1973). *Evolution of the brain and intelligence.* Academic Press.

Kalthoff, D. C. (2011). Microstructure of dental hard tissues in fossil and recent xenarthrans (Mammalia: Folivora and Cingulata). *Journal of Morphology*, *272*(6), 641–661.

Kalthoff, D. C. (2020). Short review of dental microstructure and dental microwear in xenarthran teeth. In T. Martin & W. von Koenigswald (Eds.), *Mammalian Teeth - Form and Function* (pp. 231–241). Verlag Dr. Friedrich Pfeil.

Kay, R. F., Perry, J. M. G., Malinzak, M., Allen, K. L., Kirk, E. C., Plavcan, J. M., & Fleagle, J. G. (2012). Paleobiology of Santacrucian primates. In M. S. Bargo, R. F. Kay, & S. F. Vizcaíno (Eds.), *Early Miocene Paleobiology in Patagonia: High-Latitude Paleocommunities of the Santa Cruz Formation* (pp. 306–330). Cambridge University Press.

Kay, R. F., Vizcaíno, S. F., Bargo, M. S., Spradley, J. P., & Cuitiño, J. I. (2021). Paleoenvironments and paleoecology of the Santa Cruz Formation (Early–Middle Miocene) along the Río Santa Cruz, Patagonia (Argentina). *Journal of South American Earth Sciences*, *109*, 103296.

Kerber, L., & Moraes-Santos, H. (2021). Endocranial morphology of a Middle Miocene South American dugongid and the neurosensorial evolution of Sirenians. *Journal of Mammalian Evolution*, *28*(3), 661–678.

Kraglievich, L. (1930). La Formación Friaseana (del Río Frías, Río Fénix, Laguna Blanca, etc. y su fauna de mamíferos). *Physis 10*, 127–161.

Kramarz, A. G., & Bellosi, E. S. (2005). Hystricognath rodents from the Pinturas Formation, Early–Middle Miocene of Patagonia, biostratigraphic and paleoenvironmental implications. *Journal of South American Earth Sciences*, *18*(2), 199–212.

Kramarz, A. G., & Bond, M. (2005). Los Litopterna (Mammalia) de la Formación Pinturas, Mioceno Temprano-Medio de Patagonia. *Ameghiniana*, *42*(3), 611–625.

Kramarz, A. G., Vucetich, M. G., Carlini, A. A., Ciancio, M. R., Abello, M. A., Deschamps, C. M., & Gelfo, J. N. (2010). A new mammal fauna at the top of the Gran Barranca sequence and its biochronological significance. In Madden, R. H., Carlini, A. A., Vucetich, M. G., Kay, R. F. (Eds.), *The Paleontology of Gran Barranca. Evolution and Environmental Change through the Middle Cenozoic of Patagonia* (pp. 264–277). Cambridge University Press.

Linnaeus, C. (1758). *Systema Naturae per regna tria naturae, secundum classes, ordines, genera, species, cum characteribus, differentiis, synonymis, locis.* Laurentius Salvius: Holmiae.

Marshall, L. G. (1982). Systematics of the extinct South American marsupial family Polydolopidae. *Fieldiana: Geology*, *12*, 1–109.

Marshall, L. G., & Salinas, P. (1990). Stratigraphy of the Rio Frias Formation (Miocene), along the Alto Rio Cisnes, Aisen, Chile. *Revista Geológica de Chile*, *1*(17), 57-87.

Martin, R. D. (1981). Relative brain size and basal metabolic rate in terrestrial vertebrates. *Nature 29*, 57–60.

McDonald, H. G. (2005). Paleoecology of extinct Xenarthrans and the Great American Biotic Interchange. *Bulletin of the Florida Museum of Natural History*, *45*(4), 313–333.

McGrath, A. J., Chick, J., Croft, D. A., Dodson, H. E., Flynn, J. J., & Wyss, A. R. (2022). Cavioids, chinchilloids, and erethizontoids (Hystricognathi, Rodentia, Mammalia) of the Early Miocene Pampa Castillo Fauna, Chile. *American Museum Novitates*, *3984*, 1–48.

McGrath, A. J., Flynn, J. J., Croft, D. A., Chick, J., Dodson, H. E., & Wyss, A. R. (2023). Caviomorphs (Rodentia, Hystricognathi) from Pampa Castillo, Chile: new octodontoid records and biochronological implications. *Papers in Palaeontology*, *9*(1), e1477.

McGrath, A. J., Flynn, J. J., & Wyss, A. R. (2020). Proterotheriids and macraucheniids (Litopterna: Mammalia) from the Pampa Castillo Fauna, Chile (Early Miocene, Santacrucian SALMA) and a new phylogeny of Proterotheriidae. *Journal of Systematic Palaeontology*, *18*(9), 717–738.

McKenna, M. C., Wyss, A. R., & Flynn, J. J. (2006). Paleogene pseudoglyptodont xenarthrans from central Chile and Argentine Patagonia. *American Museum Novitates*, *3536*, 1–18.

Mones, A. (1986). *Palaeovertebrata Sudamericana Catálogo Sistemático de Los Vertebrados Fósiles de America Del Sur*. Senckenbergischen Naturforschenden Gesellschaft.

Montoya-Sanhueza, G., Moreno, K., Bobe, R., Carrano, M. T., García, M., & Corgne, A. (2017). Peltephilidae and Mesotheriidae (Mammalia) from late Miocene strata of Northern Chilean Andes, Caragua. *Journal of South American Earth Sciences*, *75*, 51–65.

Muizon, C. de, & McDonald, H. G. (1995). An aquatic sloth from the Pliocene of Peru. *Nature*, *375*(6528), 224–227.

Nelson, A., Engelman, R. K., & Croft, D. A. (2023). How to weigh a fossil mammal? South American notoungulates as a case study for estimating body mass in extinct clades. *Journal of Mammalian Evolution*, *30*(3), 773–809.

Ni, X., Flynn, J. J., Wyss, A. R., & Zhang, C. (2019). Cranial endocast of a stem platyrrhine primate and ancestral brain conditions in anthropoids. *Science Advances*, *5*(8), eaav7913.

Owen, R. (1839). Fossil Mammalia. In: Darwin C (ed) *The Zoology of the Voyage of the Beagle* (pp. 13–111). Smith, Elder and Co., London.

Owen, R. (1842). *Description of the skeleton of an extinct gigantic sloth,* Mylodon robustus*, Owen: with observations on the osteology, natural affinities, and probable habits of the megatherioid quadrupeds in general.* R. and J. E. Taylor.

Peralta-Prato, J., & Solórzano, A. (2019). How many species of the aquatic sloth *Thalassocnus* (Xenarthra: Megatheriidae) were in Chile? New evidences from the Bahía Inglesa Formation, with a reappraisal of their biochronological affinities. *Andean Geology*, *46*(3), 693.

Perini, F., Macrini, T., Flynn, J. J., Bamba, K., Ni, X., Croft, D. A., & Wyss, A. R. (2022). Comparative endocranial anatomy, encephalization, and phylogeny of Notoungulata (Placentalia, Mammalia). *Journal of Mammalian Evolution*, *29*, 369–394.

Perkins, M. E., Fleagle, J. G., Heizler, M. T., Nash, B., Bown, T. M., Tauber, A. A., & Dozo, M. T. (2012). Tephrochronology of the Miocene Santa Cruz and Pinturas formations, Argentina. In M. S. Bargo, R. F. Kay, & S. F. Vizcaíno (Eds.), *Early Miocene Paleobiology in Patagonia: High-Latitude Paleocommunities of the Santa Cruz Formation* (pp. 23–40). Cambridge University Press.

Pohlenz-Kleffner, W. (1969). Vergleichende Untersuchungen zur Evolution der Gehirne von Edentaten. *Journal of Zoological Systematics and Evolutionary Research*, *7*(1), 180–208.

Pouchet, G. (1868–1869). Mémoire sur l'encéphale des Édentés. *Journal de l'Anatomie et de la Physiologie*, *5*, 658–675; *6*, 1–18, 147–162, 349–363.

Presslee, S., Slater, G. J., Pujos, F., Forasiepi, A. M., Fischer, R., Molloy, K., Mackie, M., Olsen, J. V., Kramarz, A., Taglioretti, M., Scaglia, F., Lezcano, M., Lanata, J. L., Southon, J., Feranec, R., Bloch, J., Hajduk, A., Martin, F. M., Salas Gismondi, R., . . . MacPhee, R. D. E. (2019). Palaeoproteomics resolves sloth relationships. *Nature Ecology & Evolution*, *3*(7), 1121–1130.

Pyenson, N. D., Gutstein, C. S., Parham, J. F., Le Roux, J. P., Chavarría, C. C., Little, H., Metallo, A., Rossi, V., Valenzuela-Toro, A. M., Velez-Juarbe, J., Santelli, C. M., Rogers, D. R., Cozzuol, M. A., & Suárez, M. E. (2014). Repeated mass strandings of Miocene marine mammals from Atacama Region of Chile point to sudden death at sea. *Proceedings of the Royal Society B: Biological Sciences*, *281*(1781), 20133316.

Quiñones, S. I., Zurita, A. E., Miño-Boilini, Á. R., Candela, A. M., & Luna, C. A. (2022). Unexpected record of the aquatic sloth *Thalassocnus* (Mammalia, Xenarthra, Folivora) in the upper Neogene of the Puna (Jujuy, Argentina). *Journal of Vertebrate Paleontology*, *42*(1), e2109973.

Radinsky, L. (1981). Brain evolution in extinct South American ungulates. *Brain, Behavior and Evolution*, *18*(4), 169–187.

Roberts, M., Brand, S., & Maliniak, E. (1985). The biology of captive prehensile-tailed porcupines, *Coendou prehensilis*. *Journal of Mammalogy*, *66*(3), 476–482.

Rougier, G. W., Wible, J. R., Beck, R. M. D., & Apesteguía, S. (2012). The Miocene mammal *Necrolestes* demonstrates the survival of a Mesozoic nontherian lineage into the late Cenozoic of South America. *Proceedings of the National Academy of Sciences of the United States of America*, *109*(49), 20053–20058.

Saraiva, P., & Magalhaes-Castro, B. (1975). Sensory and motor representation in the cerebral cortex of the three-toed sloth (*Bradypus tridactylus*). *Brain Research*, *90*(2), 181–193.

Scillato-Yané, G.J. (1979). Notas sobre los Dasypodidae (Mammalia, Xenarthra) del Plioceno del territorio argentino. I. Los restos de Edad Chasiquense (Plioceno inferior) del sur de la provincia de Buenos Aires: *Ameghiniana*, *14*(1–4), 133–144.

Scott, W. B. (1903). Mammalia of the Santa Cruz Beds. Volume V, Paleontology. Part I, Edentata. 2. Glyptodonta and Gravigrada. In W. B. Scott (Ed.), *Reports of the Princeton University Expeditions to Patagonia, 1896-1899* (pp. 107–226). Princeton University, E. Schweizerbart'sche Verlagshandlung (E. Nägele).

Scott, W. B. (1904). Mammalia of the Santa Cruz Beds. Volume V, Paleontology. Part I, Edentata. 3. Gravigrada. In W. B. Scott (Ed.), *Reports of the Princeton University Expeditions to Patagonia, 1896-1899* (pp. 227–364). Princeton University, E. Schweizerbart'sche Verlagshandlung (E. Nägele).

Simpson, G. (1941). A Miocene sloth from southern Chile. *American Museum Novitates*, *1156*, 1–6.

Solórzano, A., Encinas, A., Kramarz, A., Carrasco, G., Montoya-Sanhueza, G., & Bobe, R. (2021). Late Early Miocene mammals from Laguna del Laja, Cura-Mallín Formation, south-central Chile (~37°S) and their biogeographical and paleoenvironmental significance. *Journal of South American Earth Sciences*, *112*, 103544.

Stock, C. (1925). Cenozoic gravigrade edentates of western North America. *Contributions to Paleontology (Carnegie Institution of Washington)*, *331*, 1–206.

Tambusso, P. S. (2013). *Paleoneurología de xenartros fósiles* [Tesis de Maestría, Universidad de la República, Facultad de Ciencias].

Tambusso, P. S., & Fariña, R. A. (2015). Digital cranial endocast of *Pseudoplohophorus absolutus* (Xenarthra, Cingulata) and its systematic and evolutionary implications. *Journal of Vertebrate Paleontology*, *35*(5), e967853.

Tejada, J. V., Antoine, P.-O., Münch, P., Billet, G., Hautier, L., Delsuc, F., & Condamine, F. L. (2024). Bayesian total-evidence dating revisits sloth phylogeny and biogeography: a cautionary tale on morphological clock analyses. *Systematic Biology*, *73*(1), 125–139.

Tejedor, M. F. (2002). Primate canines from the Early Miocene Pinturas Formation, southern Argentina. *Journal of Human Evolution*, *43*(2), 127–141.

Toledo, N., Bargo, M. S., & Vizcaíno, S. F. (2013). Muscular reconstruction and functional morphology of the forelimb of Early Miocene sloths (Xenarthra, Folivora) of Patagonia. *The Anatomical Record*, *296*(2), 305–325.

Toledo, N., Cassini, G. H., Vizcaíno, S. F., & Bargo, M. S. (2014). Mass estimation of Santacrucian sloths from the Early Miocene Santa Cruz Formation of Patagonia, Argentina. *Acta Palaeontologica Polonica*, *59*(2), 267–280.

Varela, L., Tambusso, P. S., McDonald, H. G., & Fariña, R. A. (2019). Phylogeny, macroevolutionary trends and historical biogeography of sloths: insights from a Bayesian morphological clock analysis. *Systematic Biology*, *68*(2), 204–218.

Vizcaíno, S. F., Cassini, G. H., Fernicola, J. C., & Bargo, M. S. (2011). Evaluating habitats and feeding habits through ecomorphological features in glyptodonts (Mammalia, Xenarthra). *Ameghiniana*, *48*(3), 305–319.

Vizcaíno, S. F., Cassini, G. H., Toledo, N., & Bargo, M. S. (2012). On the evolution of large size in mammalian herbivores of Cenozoic faunas of southern South America. In B. Patterson & L. Costa (Eds.), *Bones, Clones, and Biomes: The History and Geography of Recent Neotropical Mammals* (pp. 76–101). University of Chicago Press.

Wible, J., & Rougier, G. (2017). Craniomandibular anatomy of the subterranean meridiolestidan *Necrolestes patagonensis* Ameghino, 1891 (Mammalia, Cladotheria) from the Early Miocene of Patagonia. *Annals of Carnegie Museum*, *84*, 183–252.

Woodward, A. (1900). On some remains of *Grypotherium* (*Neomylodon*) *listai* and associated mammals from a cavern near Consuelo Cove, Last Hope Inlet, Patagonia. *Proceedings of the Zoological Society of London*, *69*, 64–79.

Wyss, A. R., Flynn, J. J., & Croft, D. A. (2018). New Paleogene notohippids and leontiniids (Toxodontia; Notoungulata; Mammalia) from the early Oligocene Tinguiririca Fauna of the Andean Main Range, Central Chile. *American Museum Novitates*, *3903*, 1–42.

Wyss, A. R., Flynn, J. J., Norell, M. A., Swisher, C. C., Charrier, R., Novacek, M. J., & McKenna, M. C. (1993). South America's earliest rodent and recognition of a new interval of mammalian evolution. *Nature*, *365*(6445), 434–437.

Wyss, A. R., Flynn, J. J., Norell, M. A., Swisher, C. C., Novacek, M. J., Mckenna, M. C., & Charrier, R. (1994). Paleogene mammals from the Andes of central Chile: a preliminary taxonomic, biostratigraphic, and geochronologic assessment. *American Museum Novitates*, *3098*, 1–31.

doi: 10.5710/AMGH.26.06.2024.3603

Submitted: 28 March 2024
Accepted: 26 June 2024
Published: 08 August 2024